Theor Chim Acta (1992) 83: 69–103

Theoretica Chimica Acta

Orthogonally spin-adapted multi-reference Hilbert space coupled-cluster formalism: diagrammatic formulation*

Piotr Piecuch and Josef Paldus*****

Department of Applied Mathematics, University of Waterloo, Waterloo, Ontario, Canada N2L 3G1

Received July 3, 1991/Accepted September 25, 1991

Summary. The problem of spin-adaptation of the multi-reference (MR) coupled-cluster (CC) formalism, employing Jeziorski–Monkhorst ansatz, is addressed. The diagrammatic technique based on graphical methods of spin algebras is generalized to the MR case, so that both direct and coupling terms can be determined. Usefulness of this fully diagrammatic spin-adaptation approach is illustrated on a derivation of explicit expressions for the linear and bilinear coupling terms that are required in the special two-reference MR-CC theory involving singly and doubly excited states (MR-CCSD formalism). Results obtained with the diagrammatic approach are compared with those derived earlier using the algebraic technique and relative advantages of both procedures are compared.

Key words: Many-electron correlation problem – Coupled-cluster approach – Multi-reference formalism – Spin-adaptation – Graphical methods of spin algebras

1. Introduction

Recently, several advances have been made in the development and implementation of the so-called *Hilbert space* or *state universal* multi-reference (MR) coupled-cluster (CC) approach that is based on Jeziorski–Monkhorst cluster ansatz [1]. The explicit equations for both linear [2] and nonlinear [3] versions of the orthogonally spin-adapted MR-CC approach were derived for the special two-reference case, corresponding to a valence space spanned by two active orbitals of different symmetry. This derivation employed an algebraic approach formulated in terms of spin-free replacement operators [4], even though the resulting terms were also given a diagrammatic interpretation [3] in order to facilitate a comparison with the single-reference (SR) closed-shell case. At the same time, a diagrammatic

* To Prof. Klaus Ruedenberg at the occasion of his 70th anniversary

** *Permanent address*: Institute of Chemistry, University of Wroclaw, F. Joliot-Curie 14, 50-383 Wroclaw, Poland

*** Also affiliated with the Department of Chemistry, and Guelph-Waterloo Center for Graduate Work in Chemistry, Waterloo Campus, University of Waterloo, Waterloo, Ontario, Canada

version of the theory was developed by Meissner et al. [5, 6] for spin-orbital and non-orthogonally spin-adapted cases. The actual implementation of both approaches was tested on simple model systems investigated earlier [3, 5–8] and the approach was extended to incomplete model spaces [9].

The advantages and shortcomings of the spin-orbital vs orthogonally spin-adapted version are the same as in the SR case: The spin-orbital formalism is considerably simpler, so that it facilitates the design of more general codes which, moreover, may be more easily vectorized. It also allows the use of unrestricted Hartree–Fock (UHF) spin-orbitals which, however, should be less important in the MR than in the SR case, where the UHF spin-orbitals enable a SR handling of open-shell systems. On the other hand, the main disadvantage of the spin-orbital formalism is the necessity to handle twice as many one-electron functions and correspondingly more cluster amplitudes. The orthogonally spin-adapted version has the advantage of using the minimum number of cluster amplitudes, in addition to an obvious esthetic appeal in exploiting the spin symmetry of the Hamiltonian and a direct link with corresponding spin-adapted configuration interaction (CI) approaches and there arising CI amplitudes. This interrelationship may be very useful in actual computations of potential energy surfaces in view of a possible multitude of various solutions that the highly nonlinear MR-CC equations generally possess [8]. However, the orthogonally spin-adapted formalism is considerably more complex than the simple spin-orbital one, so that its computer implementation is more laborious and more difficult to be cast into a recursive form.

In either case, the MR formalism is much more complicated than the well known SR versions, since in addition to the so-called *direct terms*, that for each reference configuration are essentially the same as the SR equations, we also need so-called *coupling terms* [2, 3, 10], which have no counterpart in the SR case. In view of this increased complexity, one must take special precautions in order to develop an error-free formalism. Thus, to ascertain the correctness of the orthogonally spin-adapted formulation, it is desirable to carry out an independent derivation of basic equations. Relying on the diagrammatic approach [11], this is quite straightforward to achieve for the direct terms in view of their similarity with those encountered in the SR case. However, for the coupling terms, the diagrammatic technique [11] based on graphical methods of spin algebras [12] must be generalized to the MR case, involving different model space references. We present such an extension below and amply illustrate it on an independent derivation of the linear and bilinear coupling terms for the closed-shell type reference states. In particular, we independently verify the correctness of the formalism presented in [3].

The paper is organized as follows. We first recall basic definitions and notation and in Sect. 2 we generalize them to the MR case. Then, we employ the resulting formalism to derive the MR linear and bilinear coupling terms in Sect. 3 and compare the result with the algebraic derivation in the concluding Sect. 4.

2. Basic formalism

We consider two-dimensional model space [2, 3] spanned by

$$|\Phi_1\rangle = |\{(\text{core})\ {}^{(+)(-)}_{k\ k}\}\rangle \quad \text{and} \quad |\Phi_2\rangle = |\{(\text{core})\ {}^{(+)(-)}_{l\ l}\}\rangle,$$

with k and l transforming according to different irreducible representations of the spatial symmetry group of the system, $|\overset{(\pm)}{\mu}\rangle = |\mu\rangle|\frac{1}{2}, \pm\frac{1}{2}\rangle$ and curly brackets designating the antisymmetrization. The reference configurations $|\Phi_j\rangle$, $j = 1, 2$, may be interrelated as follows:

$$|\Phi_2\rangle = G^{ll}_{kk}(0)|\Phi_1\rangle, \qquad |\Phi_1\rangle = G^{kk}_{ll}(0)|\Phi_2\rangle, \tag{1}$$

where, generally,

$$G^{\varrho\sigma}_{\alpha\beta}(i) = N^{\varrho\sigma}_{\alpha\beta} S^{\varrho\sigma}_{\alpha\beta}(i), \quad i = 0, 1, \tag{2}$$

with

$$N^{\varrho\sigma}_{\alpha\beta} = [(1 + \delta_{\alpha\beta})(1 + \delta^{\varrho\sigma})]^{-\frac{1}{2}}, \tag{2'}$$

and

$$S^{\varrho\sigma}_{\alpha\beta}(i) = [i]^{-\frac{1}{2}} \sum_{m_\alpha, m_\beta, m^\varrho, m^\sigma} \sum_{m} \langle \tfrac{1}{2} m_\alpha, \tfrac{1}{2} m_\beta | im \rangle \langle \tfrac{1}{2} m^\varrho, \tfrac{1}{2} m^\sigma | im \rangle X^{\varrho m^\varrho} X_{\alpha m_\alpha} X^{\sigma m^\sigma} X_{\beta m_\beta}, \tag{2''}$$

represents a particle-particle–hole-hole (*pp-hh*) coupled orthogonally spin-adapted biexcitation operator [13]. We employ a convention designating the dimension of the spin space $(2S + 1)$ by $[S]$, i.e. $[X] \equiv 2X + 1$ for any spin quantum number X. The corresponding monoexcitation operator is then:

$$G^\varrho_\alpha = S^\varrho_\alpha = 2^{-\frac{1}{2}} X^{\varrho m} X_{\alpha m}. \tag{3}$$

We write $X^{\kappa m} \equiv X^\dagger_{\kappa m}$ and use Einstein summation convention to indicate unrestricted summation over repeated upper and lower indices [e.g., m in Eq. (3)]. Occupied orbitals in the reference state, chosen as a Fermi vacuum (in most cases $|\Phi_1\rangle$), are labeled by $\alpha, \beta, \ldots$, while the unoccupied ones by $\varrho, \sigma, \ldots$. Core orbitals are labeled by $a, b, \ldots$, virtual orbitals by $r, s, \ldots$, and the labels $\kappa, \lambda, \ldots$ are employed as generic indices that run over all (occupied and unoccupied, or, core, valence and virtual) orbitals (cf. Table 1 of [2]). In addition to fixed valence labels k and l, we also employ free (summation) [14] valence labels k', k'' and l', l'', which in the two-reference case assume a single value, $k' = k'' = k$, $l' = l'' = l$. We also note that formally

$$\begin{aligned} S^\alpha_\varrho &= (S^\varrho_\alpha)^\dagger, \\ S^{\alpha\beta}_{\varrho\sigma}(i) &= [S^{\varrho\sigma}_{\alpha\beta}(i)]^\dagger, \\ N^{\alpha\beta}_{\varrho\sigma} &= N^{\varrho\sigma}_{\alpha\beta} = (N^{\alpha\beta}_{\varrho\sigma})^*, \end{aligned} \tag{4}$$

so that we may define

$$G^\alpha_\varrho \equiv (G^\varrho_\alpha)^\dagger, \tag{5a}$$

$$G^{\alpha\beta}_{\varrho\sigma}(i) \equiv [G^{\varrho\sigma}_{\alpha\beta}(i)]^\dagger. \tag{5b}$$

In particular,

$$G^{kk}_{ll}(0) = [G^{ll}_{kk}(0)]^\dagger. \tag{6}$$

When the cubic and higher-order terms in cluster amplitudes are nelgected, the coupling term Λ_c (cf. [1]),

$$\Lambda_c \equiv \langle {}^{(p)}G_i \Phi_p | \, e^{-T^{(p)}} e^{T^{(q)}} | \Phi_q \rangle H^{\text{eff}}_{qp}, \quad q = 3 - p, p = 1, 2, \tag{7}$$

can be written as

$$\begin{aligned} \Lambda_c = {} & \langle {}^{(p)}G_i \Phi_p | T^{(q)} - T^{(p)} | \Phi_q \rangle H^{\text{eff}}_{qp} \\ & + \tfrac{1}{2} \langle {}^{(p)}G_i \Phi_p | (T^{(q)} - T^{(p)})^2 + [T^{(q)}, T^{(p)}] | \Phi_q \rangle H^{\text{eff}}_{qp}, \end{aligned} \tag{8}$$

or

$$\Lambda_c = \langle {}^{(p)}G_i\Phi_p | T^{(q)} - T^{(p)} | \Phi_q \rangle H_{qp}^{\text{eff}} + \tfrac{1}{2}\langle {}^{(p)}G_i\Phi_p | T^{(q)2} + T^{(p)2} - 2T^{(p)}T^{(q)} | \Phi_q \rangle H_{qp}^{\text{eff}}. \tag{9}$$

Here

$$H_{qp}^{\text{eff}} = \langle \Phi_q | e^{-T^{(p)}} H e^{T^{(p)}} | \Phi_p \rangle \tag{10}$$

$$= \langle \Phi_q | (H_{N_p} e^{T^{(p)}})_C | \Phi_p \rangle \tag{11}$$

is the effective Hamiltonian matrix element and ${}^{(p)}G_i$ designates a spin-adapted singlet excitation operator, Eqs. (2), (3), that generates excitations *outside* the model space. This excludes operators like ${}^{(1)}G_k^l$ or ${}^{(1)}G_{kk}^{ll}(0)$. The superscript (p) in ${}^{(p)}G_i$ indicates that the excitation operator is defined with respect to the reference $|\Phi_p\rangle$ and the subscript C designates the connected component. Similarly, the subscript N_p in H_{N_p} designates the normal product form of H (cf. [14]) defined relative to $|\Phi_p\rangle$. Clearly, H_{qp}^{eff} depends only on the valence indices that distinguish $|\Phi_p\rangle$ and $|\Phi_q\rangle$. For example,

$$H_{21}^{\text{eff}} = \langle \Phi_2 | (H_{N_1} e^{T^{(1)}})_C | \Phi_1 \rangle = \langle \Phi_1 | {}^{(1)}G_{ll}^{kk}(0)(H_{N_1} e^{T^{(1)}})_C | \Phi_1 \rangle \equiv g_{ll}^{kk}, \tag{12}$$

where in the last identity we employed the notation of [3] [Eq. (21)]. Similarly,

$$H_{12}^{\text{eff}} = \langle \Phi_2 | {}^{(2)}G_{kk}^{ll}(0)(H_{N_2} e^{T^{(2)}})_C | \Phi_2 \rangle \equiv g_{kk}^{ll}. \tag{13}$$

Of course, matrix elements H_{qp}^{eff} in Eqs. (8) and (9) are sometimes replaced by truncated quantities, like $H_{qp} = \langle \Phi_q | H_{N_p} | \Phi_p \rangle$ or by $\langle \Phi_q | H + [H, T^{(p)}] | \Phi_p \rangle = \langle \Phi_q | [H_{N_p}(1 + T^{(p)})]_C | \Phi_p \rangle$. In order to parallel the results obtained with the algebraic approach [2, 3], we shall rely on Eq. (8), although Eq. (9) will also prove to be useful (cf. Sect. 4).

We employ the CCSD approximation, i.e.:

$$T^{(p)} = T_1^{(p)} + T_2^{(p)}, \tag{14}$$

where, in the orthogonally spin-adapted formalism,

$$T_1^{(p)} = \sum_{\alpha\varrho} \langle \varrho | t_1^{(p)} | \alpha \rangle {}^{(p)}G_\alpha^\varrho \tag{15}$$

$$= {}^{(p)}t_\varrho^\alpha \, {}^{(p)}S_\alpha^\varrho, \tag{16}$$

$$T_2^{(p)} = \sum_{\substack{\alpha \leqslant \beta \\ \varrho \leqslant \sigma}} \sum_{i=0}^{1} \langle \varrho\sigma | t_2^{(p)} | \alpha\beta \rangle_i {}^{(p)}G_{\alpha\beta}^{\varrho\sigma}(i) \tag{17}$$

$$= \tfrac{1}{4} \sum_{i=0}^{1} {}^{(p)}t_{\varrho\sigma}^{\alpha\beta}(i) \, {}^{(p)}S_{\alpha\beta}^{\varrho\sigma}(i) \tag{18}$$

with

$${}^{(p)}t_{\varrho\sigma}^{\alpha\beta}(i) = N_{\alpha\beta}^{\varrho\sigma} \langle \varrho\sigma | t_2^{(p)} | \alpha\beta \rangle_i. \tag{19}$$

Choosing $|\Phi_p\rangle$ as a Fermi vacuum, we can represent the operators $T_i^{(p)}$, $i = 1, 2$, Eqs. (15)–(18), by Hugenholtz vertices whose nonoriented form is shown in Fig. 1a,b. Similar diagrams can be used to represent excitation operators (2) or (2″) and (3). To make the distinction, we shall use a filled circle in the latter case. The diagrammatic representation for the operator Ω_p^q

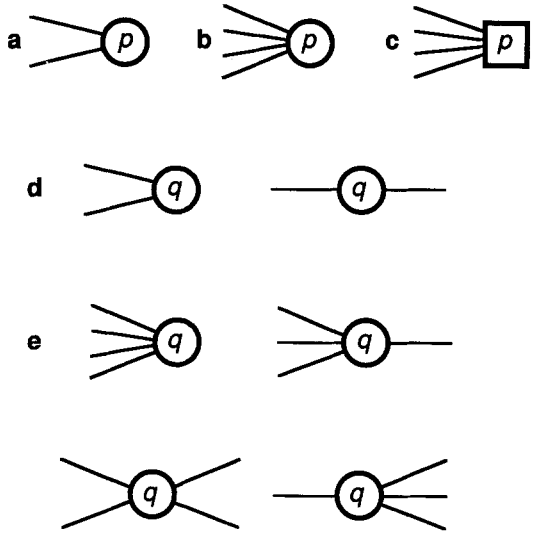

Fig. 1a–e. Nonoriented Hugenholtz vertices representing the operators $T_1^{(p)}$ (diagram a), $T_2^{(p)}$ (diagram b) and Ω_p^q (diagram c) as well as $T_1^{(q)}$ (diagram d) and $T_2^{(q)}$ (diagram e), when Φ_p is chosen as a Fermi vacuum

that transforms $|\Phi_p\rangle$ into $|\Phi_q\rangle$, i.e.,

$$\Omega_1^2 = G_{kk}^{ll}(0), \qquad \Omega_2^1 = G_{ll}^{kk}(0), \tag{20}$$

is shown in Fig. 1c. Although in the diagrams a, b and c of Fig. 1 all the lines extend to the left, there is an essential difference between them. According to general MR-CC formalism [1], cluster amplitudes must carry at least one non-valence (i.e. core or virtual-type) index. Thus, at least one line of diagrams representing $T_i^{(p)}$, $i = 1, 2$, must be of a non-valence type, while all the lines in the Ω_p^q diagram, Fig. 1c, carry valence indices. Using the MR-MBPT terminology, diagrams representing $T_i^{(p)}$, $i = 1, 2$, operators are *open* while that for Ω_p^q is *closed.* Representing valence lines by double arrows, we thus have that

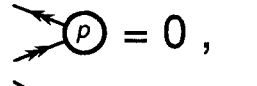

(21)

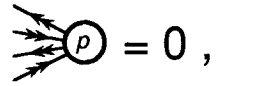

(22)

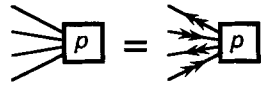

(23)

In other words, the resulting diagrams, in which all the lines that are incident with $T_i^{(p)}$, $i = 1, 2$, vertices are of the valence type, must vanish.

Notice that the diagram of Fig. 1c can also represent the operator $\tilde{T}_2^{(p)}$ [cf. Eq. (27) of [3]],

$$\tilde{T}_2^{(p)} = H_{qp}^{\text{eff}} \Omega_p^q, \tag{24}$$

that describes an excitation inside the model space, in contrast to operators $T_i^{(p)}$, creating excitations into the orthogonal complement of (i.e., outside) the model

space. This operator is closely related with the effective Hamiltonian

$$^{(p)}H^{\text{eff}} = PHUP_p, \tag{25}$$

or the effective interaction

$$^{(p)}W^{\text{eff}} = PH_{N_p}UP_p, \tag{26}$$

and can be written explicitly as follows (summation convention does not apply here since k and l are fixed):

$$\tilde{T}_2^{(1)} = g_{ll}^{kk} G_{kk}^{ll}(0), \tag{27}$$

$$\tilde{T}_2^{(2)} = g_{kk}^{ll} G_{ll}^{kk}(0). \tag{28}$$

Here,

$$P = P_1 + P_2, \qquad P_p = |\Phi_p\rangle\langle\Phi_p|, \quad p = 1, 2, \tag{29}$$

and

$$U = e^{T^{(1)}}P_1 + e^{T^{(2)}}P_2 \tag{30}$$

is the usual Bloch wave operator [1]. For example,

$$^{(p)}H^{\text{eff}} = H_{pp}^{\text{eff}}P_p + \tilde{T}_2^{(p)}P, \tag{31}$$

where [cf. Eqs. (10) and (11)]

$$\begin{aligned} H_{pp}^{\text{eff}} &= \langle\Phi_p| e^{-T^{(p)}} H e^{T^{(p)}} |\Phi_p\rangle \\ &= H_{pp} + \langle\Phi_p|(H_{N_p} e^{T^{(p)}})_C|\Phi_p\rangle. \end{aligned} \tag{32}$$

To derive Eq. (31), we have to realize that

$$\Omega_p^q|\Phi_q\rangle = 0, \tag{33}$$

so that

$$\tilde{T}_2^{(p)}P = H_{qp}^{\text{eff}}\Omega_p^q(P_p + P_q) = H_{qp}^{\text{eff}}|\Phi_q\rangle\langle\Phi_p|. \tag{34}$$

It is thus not surprising that diagrammatic representations of $\tilde{T}_2^{(p)}$, and of operators (25) or (26), are similar [5, 6].

Clearly, the diagrams representing conjugate excitation operators $^{(p)}G_\varrho^\alpha$ or $^{(p)}S_\varrho^\alpha$ and $^{(p)}G_{\varrho\sigma}^{\alpha\beta}(i)$ or $^{(p)}S_{\varrho\sigma}^{\alpha\beta}(i)$, Eqs. (4), (5), are conjugate to those of Fig. 1a,b. It thus remains to draw the diagrams which represent the cluster operators $T_i^{(q)}$ ($i = 1, 2$), when Φ_p ($p \neq q$) is chosen as a Fermi vacuum. We can use the same type of vertices as shown in Fig. 1a (for $i = 1$) and 1b (for $i = 2$). Clearly, they must be labeled with q instead of p and, in contrast to diagrams representing $T_i^{(p)}$, the fermion lines may now extend to the left as well as to the right (see Fig. 1d,e). Since all the lines that extend to the right carry valence labels that distinguish Φ_p and Φ_q, at least one line incident with $T_i^{(q)}$ vertex must extend to the left, lest the diagram vanishes (cf. Fig. 1d,e). Otherwise, contrary to the results of the general MR-CC formalism [1], the cluster operators $T_i^{(q)}$ would produce excitations into the model space.

Equipped with this diagrammatic representation, we find that within the realm of the CCSD approximation (i.e., considering only singly and doubly excited configurations relative to a given reference), only a few terms in Eqs. (8) and (9) survive. For example, the linear term $\langle^{(p)}G_i\Phi_p|T^{(p)}|\Phi_q\rangle H_{qp}^{\text{eff}}$, which is represented by diagrams resulting from one skeleton of Fig. 1a,b and the

skeleton of Fig. 1c, must vanish unless ${}^{(p)}G_i$ represents a triexcitation (for the $T_1^{(p)}$ component) or a tetraexcitation (for the $T_2^{(p)}$ component) operator, since no lines of $T_i^{(p)}$ and Ω_p^q can be contracted (see also Table 3 of [2]). Thus, since we restrict ourselves to singly and doubly excited cluster components, Eq. (14), this term will vanish as does the quadratic term in $T^{(p)}$. We also see easily that from $\langle {}^{(p)}G_i\Phi_p|T^{(q)}T^{(p)}|\Phi_q\rangle$ and $\langle {}^{(p)}G_i\Phi_p|T^{(p)}T^{(q)}|\Phi_q\rangle$ terms, only the terms involving $T_2^{(q)}$ and $T_1^{(p)}$ survive, assuming that $G_i^{(p)}$ represents at most a double excitation [cf. diagrams in Fig. 11d and h in Sect. 3]. We thus find that the coupling term Λ_c, Eq. (8), can be rewritten in the form:

$$\Lambda_c = \sum_{n=1}^{2} R_n^{(p)}(G_i^\dagger) + \sum_{\substack{n,n'=1 \\ (n\leqslant n')}}^{2} B_{nn'}^{(p)}(G_i^\dagger) + \tilde{B}_{12}^{(p)}(G_i^\dagger), \tag{35}$$

where

$$R_n^{(p)}(G_i^\dagger) = \langle\Phi_p|{}^{(p)}G_i^\dagger T_n^{(q)}|\Phi_q\rangle H_{qp}^{\text{eff}}, \tag{36}$$

$$B_{nn}^{(p)}(G_i^\dagger) = \tfrac{1}{2}\langle\Phi_p|{}^{(p)}G_i^\dagger T_n^{(q)2}|\Phi_q\rangle H_{qp}^{\text{eff}}, \tag{37}$$

$$B_{12}^{(p)}(G_i^\dagger) = \langle\Phi_p|{}^{(p)}G_i^\dagger T_2^{(q)}(T_1^{(q)} - T_1^{(p)})|\Phi_q\rangle H_{qp}^{\text{eff}}, \tag{38}$$

$$\tilde{B}_{12}^{(p)}(G_i^\dagger) = \langle\Phi_p|{}^{(p)}G_i^\dagger [T_2^{(q)}, T_1^{(p)}]|\Phi_q\rangle H_{qp}^{\text{eff}}, \tag{39}$$

while Eq. (9) becomes:

$$\Lambda_c = \sum_{n=1}^{2} R_n^{(p)}(G_i^\dagger) + \sum_{n=1}^{2} B_{nn}^{(p)}(G_i^\dagger) + \tilde{\tilde{B}}_{12}^{(p)}(G_i^\dagger), \tag{40}$$

where

$$\tilde{\tilde{B}}_{12}^{(p)}(G_i^\dagger) = \langle\Phi_p|{}^{(p)}G_i^\dagger (T_1^{(q)} - T_1^{(p)})T_2^{(q)}|\Phi_q\rangle H_{qp}^{\text{eff}}. \tag{41}$$

Equivalence of Eqs. (35) and (40) is obvious, since

$$\tilde{\tilde{B}}_{12}^{(p)}(G_i^\dagger) = B_{12}^{(p)}(G_i^\dagger) + \tilde{B}_{12}^{(p)}(G_i^\dagger). \tag{42}$$

Although Eq. (40) is simpler, Eq. (35) is more convenient when the algebraic approach based on the E-operator technique [2–4] is employed. Eq. (35) can be rewritten in terms of commutators, which can be evaluated using the contraction theorem [15] or analogous rules. This is why Eq. (35) was used in [3] that relied on the algebraic approach. Another reason for splitting of $\tilde{\tilde{B}}_{12}^{(p)}$ into $B_{12}^{(p)}$ and $\tilde{B}_{12}^{(p)}$, Eq. (42), will be given later. On the other hand, Eq. (40) is more convenient in the diagrammatic approach, since it contains fewer terms to evaluate. Nonetheless, we shall use Eq. (35), since we wish to compare the diagrammatic method with the algebraic replacement operator technique [2–4] of spin-adaptation.

We can limit ourselves to Eqs. (35) and (40) for $p = 1$. Corresponding expressions for $p = 2$ easily follow from the former ones if we interchange indices k and l and the amplitudes of $T^{(1)}$ and $T^{(2)}$. To derive explicit expressions for the R, B and $\tilde{B}$ terms in Eq. (35) for $G_i = G_\alpha^a$ and $G_{\alpha\beta}^{a\sigma}(i)$, $i = 0, 1$, using a diagrammatic technique [11, 13b] based on graphical methods of spin algebras [12], we first introduce orbital and spin diagrams representing basic quantities (operators) in Eqs. (36)–(39), as indicated in Figs. 2 and 3. Brandow-type orbital diagrams representing cluster operators $T_i^{(1)}$, $i = 1, 2$, with $|\Phi_1\rangle$ as a Fermi vacuum, are shown in Fig. 2a and c, while those representing $T_i^{(2)}$, $i = 1, 2$, components are displayed in Fig. 3. Formally, all the orbital and intermediate spin labels are free, including valence labels k', k'', l' and l'' in Fig. 3. Of course,

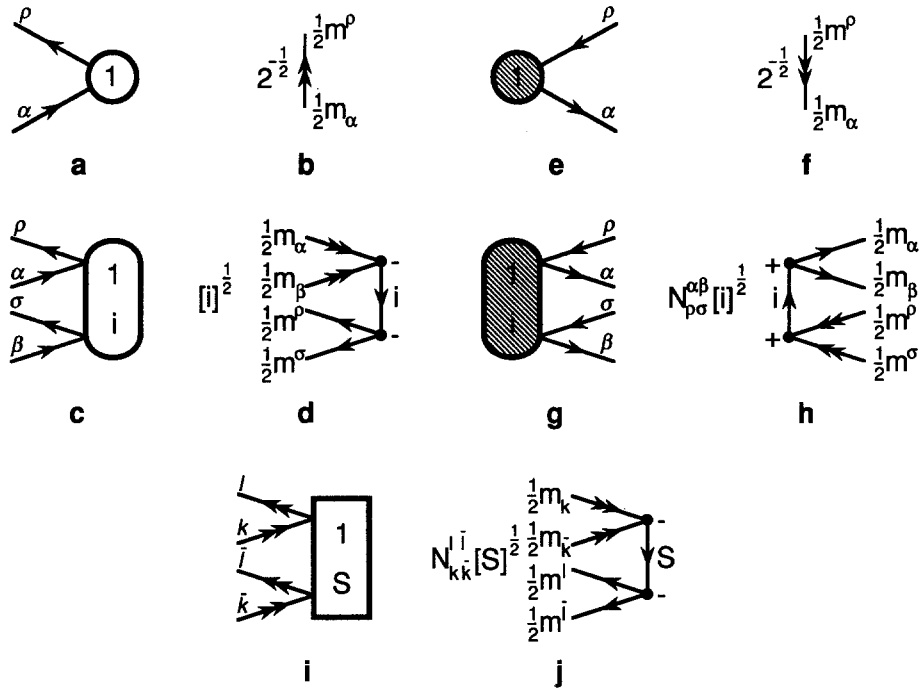

Fig. 2a–j. Diagrammatic representation of the operators $T_1^{(1)}$, Eq. (16) [diagrams a, b], $T_2^{(1)}$, Eq. (18) [diagrams c, d], ${}^{(1)}G_\varrho^\alpha$, Eq. (5a) [diagrams e, f], ${}^{(1)}G_{\varrho\sigma}^{\alpha\beta}(i)$, Eq. (5b) [diagrams g, h], and ${}^{(1)}G_{k\bar{k}}^{ll}(S)$ [diagrams i, j]. Diagrams a, c, e, g and i represent a Brandow-type version of nonoriented Hugenholtz vertices of Fig. 1a–c, while b, d, f, h and j are the corresponding 3-*jm*-type spin diagrams

in the final expressions pertaining to the two-reference case considered earlier [2, 3] we have to set $k' = k'' = k$ and $l' = l'' = l$, since there is only one valence orbital (k) occupied in $|\Phi_1\rangle$ and unoccupied in $|\Phi_2\rangle$ and, similarly, one valence orbital (l) unoccupied in $|\Phi_1\rangle$ and occupied in $|\Phi_2\rangle$. The 3-*jm*-type spin diagrams associated with $T_i^{(p)}$ ($i = 1, 2$; $p = 1, 2$) diagrams are shown in Fig. 2b and d. The diagrams a and b of Fig. 2 can also serve to represent the single excitation operators ${}^{(1)}S_\alpha^\varrho$ or ${}^{(1)}G_\alpha^\varrho$, Eq. (3), provided that the orbital and spin labels are fixed. Likewise, diagrams c and d of Fig. 2 can be used to represent double excitation operators ${}^{(1)}S_{\alpha\beta}^{\varrho\sigma}(i)$, Eq. (2″), or ${}^{(1)}G_{\alpha\beta}^{\varrho\sigma}(i)$, Eq. (2), assuming that the normalization factor $N_{\alpha\beta}^{\varrho\sigma}$ is incorporated into the spin graph, Fig. 2d. Corresponding conjugate diagrams e and g of Fig. 2 and associated spin graphs f and h of Fig. 2 serve to represent conjugate excitation operators, Eq. (5). As already mentioned, we use filled vertices for excitation operators. Finally, we need a graphical representation for the operator ${}^{(1)}G_{kk}^{ll}(0) \equiv G_{kk}^{ll}(0)$ transforming $|\Phi_1\rangle$ into $|\Phi_2\rangle$. For combinatorial reasons it is prudent to consider a more general operator ${}^{(1)}G_{k\bar{k}}^{ll}(S)$, and set in the final expressions $k = \bar{k}$, $l = \bar{l}$ and $S = 0$. The Brandow orbital diagram and the corresponding 3-*jm* graph representing ${}^{(1)}G_{k\bar{k}}^{ll}(S)$ operator are shown in Fig. 2i and j, respectively.

Rather than considering the R, B and $\tilde{B}$ terms in Eqs. (35)–(39), with $p = 1$, as matrix elements between $\langle {}^{(1)}G_i\Phi_1|$ and $|{}^{(1)}G_{kk}^{ll}(0)\Phi_1\rangle$ that must be subsequently multiplied by $H_{21}^{\text{eff}} = g_{ll}^{kk}$, we can also express them via the operator $\tilde{T}_2^{(1)}$,

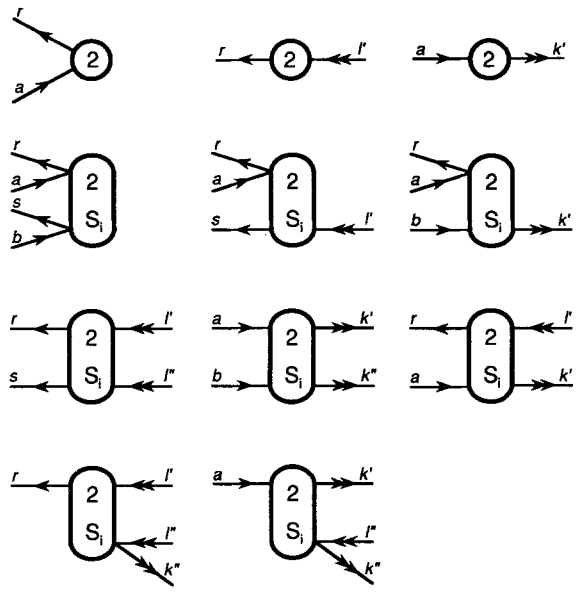

Fig. 3a,b. Possible Brandow-type orbital diagrams representing $T_1^{(2)}$ (a) and $T_2^{(2)}$ (b), with Φ_1 chosen as a Fermi vacuum, corresponding to nonoriented Hugenholtz vertices of Fig. 1d and e, respectively. Scalar factors associated with diagrams a are ${}^{(2)}t_r^a$, ${}^{(2)}t_{r'}^{l'}$ and ${}^{(2)}t_{k'}^{a}$, respectively, and scalar factors associated with b are ${}^{(2)}t_{rs}^{ab}(S_i)$, ${}^{(2)}t_{rs}^{al'}(S_i)$, ${}^{(2)}t_{rk'}^{ab}(S_i)$, ${}^{(2)}t_{rs}^{l'l''}(S_i)$, ${}^{(2)}t_{k'k''}^{ab}(S_i)$, ${}^{(2)}t_{k'r}^{al'}(S_i)$, ${}^{(2)}t_{rk''}^{l'l''}(S_i)$, and ${}^{(2)}t_{k'k''}^{al''}(S_i)$, respectively. In the final formulas, we have to set $k' = k'' = k$ and $l' = l'' = l$. We do not present corresponding spin diagrams, since they are identical with those given in Fig. 2b [for diagrams of part a] and Fig. 2d [for diagrams of part b]

Eq. (27), which can be written as

$$\tilde{T}_2^{(1)} = \tfrac{1}{4} \sum_S {}^{(1)}\gamma_{ll'}^{kk''}(S)\, {}^{(1)}S_{kk''}^{ll''}(S), \tag{43}$$

where k', k'', l', l'' and S are free summation labels and

$${}^{(1)}\gamma_{ll''}^{kk''}(S) = \delta_k^{k'}\delta_k^{k''}\delta_l^{l}\delta_{l'}^{l}\delta_{S,0}(N_{kk}^{ll})^{-1} g_{ll}^{kk}. \tag{44}$$

Indeed,

$$R_n^{(1)}(G_i^\dagger) = \langle \Phi_1 | {}^{(1)}G_i^\dagger T_n^{(2)} \tilde{T}_2^{(1)} | \Phi_1 \rangle, \tag{45}$$

$$B_{nn}^{(1)}(G_i^\dagger) = \tfrac{1}{2} \langle \Phi_1 | {}^{(1)}G_i^\dagger T_n^{(2)2} \tilde{T}_2^{(1)} | \Phi_1 \rangle, \tag{46}$$

$$B_{12}^{(1)}(G_i^\dagger) = \langle \Phi_1 | {}^{(1)}G_i^\dagger T_2^{(2)} (T_1^{(2)} - T_1^{(1)}) \tilde{T}_2^{(1)} | \Phi_1 \rangle, \tag{47}$$

$$\tilde{B}_{12}^{(1)}(G_i^\dagger) = \langle \Phi_1 | {}^{(1)}G_i^\dagger [T_2^{(2)}, T_1^{(1)}] \tilde{T}_2^{(1)} | \Phi_1 \rangle. \tag{48}$$

Expressions (45)–(48) can be directly evaluated once we choose a suitable graphical representation of the operator $\tilde{T}_2^{(1)}$, Eq. (43). To this end we can use diagrams i and j of Fig. 2, provided that we replace fixed orbital labels k, $\bar{k}$ by free ones k', k'', regard spin label S as a summation index and remove the factor $N_{kk''}^{ll''}$ from the spin graph in Fig. 2j. The scalar factor associated with a modified orbital diagram, Fig. 2i, is then ${}^{(1)}\gamma_{ll''}^{kk''}(S)$, Eq. (44). Thus, the coefficients (44) play now the same role as the unnormalized pair-cluster amplitudes ${}^{(p)}t_{q\sigma}^{\alpha\beta}(i)$, Eq. (18).

We can thus find the explicit expressions for R, B and $\tilde{B}$ terms by either using Eqs. (45)–(48) with $\tilde{T}_2^{(1)}$ given by Eq. (43), or by using Eqs. (36)–(39) and

evaluating the matrix elements between $\langle {}^{(1)}G_i\Phi_1|$ and $|G^{ll}_{kk}(0)\Phi_1\rangle$. Although both methods must yield the same result (cf. the next section), the latter one is slightly more convenient, since in the resulting Brandow diagrams we do not have to draw vertices representing ${}^{(1)}G^{\dagger}_i$ and $G^{ll}_{kk}(0)$ operators. When Eqs. (45)–(48) are employed, vertices representing the $\tilde{T}^{(1)}_2$ operator must be drawn.

3. Diagrammatic evaluation of the coupling term

When deriving the explicit form of the coupling term Λ_c, we need the expression for g^{kk}_{ll}, Eq. (12), assuming that $T^{(1)} = T^{(1)}_1 + T^{(1)}_2$. This was already accomplished in [16], where we found that

$$g^{kk}_{ll} = N^{ll}_{kk}\langle\Phi_1|{}^{(1)}S^{kk}_{ll}(0)(H_{N_1}e^{T^{(1)}_1+T^{(1)}_2})_C|\Phi_1\rangle = \tfrac{1}{2}\sum_{j=0}^{4}{}^{(j)}\Lambda^{kk}_{ll}(0). \tag{49}$$

The explicit expressions for the quantities ${}^{(j)}\Lambda^{\alpha\beta}_{\varrho\sigma}(i)$ are also given in [16], (cf. Eqs. (57)–(61) of [16]). Different truncation schemes for the expansion (49) will lead to different versions of the quadratic two-reference CCSD formalism considered in this paper, since both the matrix element of the product $e^{-T^{(1)}}e^{T^{(2)}}$ between $\langle {}^{(1)}G_i\Phi_1|$ and $|\Phi_2\rangle = |G^{ll}_{kk}(0)\Phi_1\rangle$ (see Eq. (7)) and the effective Hamiltonian matrix element H^{eff}_{21} contain higher than linear terms in cluster amplitudes. We may, for example, consider the theory in which the entire coupling term is at most bilinear in cluster coefficients. In such a case, we only need those parts of ${}^{(j)}\Lambda^{kk}_{ll}(0)$ that are at most linear in cluster amplitudes (see Eqs. (8) and (9) or (35)–(41)), so that $j=3$ and $j=4$ terms in Eq. (49) do not contribute and, consequently (see [16]),

$$\begin{aligned} g^{kk}_{ll} = {} & v^{kk}_{ll} + 2^{\frac{1}{2}}(v^{\varrho k}_{ll}\,{}^{(1)}t^{k}_{\varrho} - v^{kk}_{\alpha l}\,{}^{(1)}t^{\alpha}_{l}) + {}^{(1)}f^{\varrho}_{l}\,{}^{(1)}t^{kk}_{\varrho l}(0) - {}^{(1)}f^{k}_{\alpha}\,{}^{(1)}t^{\alpha k}_{ll}(0) \\ & + \tfrac{1}{2}[v^{\varrho\sigma}_{ll}\,{}^{(1)}t^{kk}_{\varrho\sigma}(0) + v^{kk}_{\alpha\beta}\,{}^{(1)}t^{\alpha\beta}_{ll}(0)] + v^{\varrho k}_{\alpha l}[{}^{(1)}t^{k\alpha}_{l\varrho}(0) + 3^{\frac{1}{2}}\,{}^{(1)}t^{k\alpha}_{l\varrho}(1)] - 2v^{k\varrho}_{\alpha l}\,{}^{(1)}t^{k\alpha}_{l\varrho}(0), \end{aligned} \tag{50}$$

where

$${}^{(1)}f^{\lambda}_{\kappa} = z^{\lambda}_{\kappa} + (2v^{\lambda\alpha}_{\kappa\alpha} - v^{\alpha\lambda}_{\kappa\alpha}), \tag{51}$$

(α runs here over the orbitals occupied in $|\Phi_1\rangle$), and $z^{\lambda}_{\kappa} = \langle\kappa|z|\lambda\rangle$ and $v^{\mu\nu}_{\kappa\lambda} = \langle\kappa\lambda|v|\mu\nu\rangle$ are, respectively, standard one- and two-electron integrals. The whole expression (50) then enters $R^{(1)}_n(G^{\dagger}_i)$, while only the constant part of it (i.e., the term v^{kk}_{ll}) enters $B^{(1)}_{nn'}(G^{\dagger}_i)$ and $\tilde{B}^{(1)}_{12}(G^{\dagger}_i)$. We can also consider a higher level formalism, in which in calculating R, B and $\tilde{B}$ terms the entire expansion (49) (containing even quartic contributions in cluster amplitudes; cf. [16]) is used. Finally, we can consider an intermediate version, in which we include at most bilinear terms in both the matrix element of the product $e^{-T^{(1)}}e^{T^{(2)}}$ and the effective Hamiltonian matrix element H^{eff}_{21}. All these versions are based on the same formula for Λ_c, Eq. (35) or (40), and in all of them the explicit expressions for ${}^{(j)}\Lambda^{\alpha\beta}_{\varrho\sigma}(i)$, which were derived in [16], apply.

Now, to apply the diagrammatic procedure [11, 13b] to Eqs. (36)–(39) with $p=1$, or Eqs. (45)–(48), we must first draw all possible nonequivalent, nonoriented vacuum Hugenholtz skeletons that can be formed from the vertices representing the operators ${}^{(1)}G^{\alpha}_{\varrho}$ or ${}^{(1)}G^{\alpha\beta}_{\varrho\sigma}(i)$, $G^{ll}_{kk}(0)$ or $\tilde{T}^{(1)}_2$, and the pertinent products of cluster operators. Once this is done, we have to introduce orienta-

tions and labeling of lines in all nonequivalent ways. Then, each Hugenholtz vertex is replaced by its Brandow version, yielding the orbital diagrams, and, finally, the corresponding spin diagrams are constructed. The desired final expressions are then obtained by combining the resulting spin-coupling coefficients (determined by exploiting the graphical methods of spin algebras [12]) with the orbital factors.

As mentioned earlier, there are at least two possible strategies to follow: we can either calculate the matrix elements between $\langle {}^{(1)}G_i\Phi_1|$ and $|G^{ll}_{kk}(0)\Phi_1\rangle$, corresponding to Eqs. (36)–(39), or use Eqs. (45)–(48) with $\tilde{T}_2^{(1)}$ defined by Eq. (43). Let us illustrate these two possibilities on a typical example, considering $\tilde{B}^{(1)}_{12}[G^{\alpha\beta}_{\varrho\sigma}(i)]$, Eq. (39) or (48). Instead of the matrix element $\langle\Phi_1|{}^{(1)}G^{\alpha\beta}_{\varrho\sigma}(i)[T_2^{(2)}, T_1^{(1)}]G^{ll}_{kk}(0)|\Phi_1\rangle$ we consider a more general one, namely

$$B \equiv \langle\Phi_1|{}^{(1)}G^{\alpha\beta}_{\varrho\sigma}(i)[T_2^{(2)}, T_1^{(1)}]\,{}^{(1)}G^{ll}_{k\bar{k}}(S)|\Phi_1\rangle, \tag{52}$$

which would be needed when more than two active orbitals were involved. To evaluate B, Eq. (52), we have to draw four Hugenholtz diagrams, whose Brandow form will be given later (cf. Fig. 12a–d), when all the coupling terms are systematically evaluated. One of these diagrams (cf. Fig. 12a) gives the contribution:

$$2^{-\frac{1}{2}}\delta_{iS}[S]^{-\frac{1}{2}}N^{\alpha\beta}_{\varrho\sigma}N^{ll}_{k\bar{k}}\mathscr{S}^{ll}(S)\{\delta^l_\varrho\delta^{\bar{l}}_\sigma\}\mathscr{S}^{\alpha\beta}(i)\{{}^{(1)}t^{\alpha\,(2)}_{l'}t^{\beta l'}_{k\bar{k}}(S)\}, \tag{53'}$$

which for $k=\bar{k}$, $l=\bar{l}=l'$ and $S=0$ (the case considered in this paper) equals (cf. Eq. (109))

$$2^{-\frac{1}{2}}\delta_{i0}N^{\alpha\beta}_{\varrho\sigma}\delta^l_\varrho\delta^l_\sigma\mathscr{S}^{\alpha\beta}\,{}^{(1)}t^{\alpha\,(2)}_{l}t^{\beta l}_{k\bar{k}}(0). \tag{53}$$

Note that the corresponding spin graph (see the Appendix, Table 3) gives the factor $2^{-\frac{1}{2}}\delta_{iS}[S]^{-\frac{1}{2}}$, which, due to the presence of the normalized bra and ket states in Eq. (52), is multiplied by $N^{\alpha\beta}_{\varrho\sigma}$ and $N^{ll}_{k\bar{k}}$. The weight of the diagram equals to one. Further, $\mathscr{S}^{\kappa\lambda}(i)$ is a two-index symmetrizer ($i=0$) or antisymmetrizer ($i=1$),

$$\mathscr{S}^{\kappa\lambda}(i) \equiv \mathscr{S}_{\kappa\lambda}(i) = 1 + (-1)^i(\kappa\lambda), \tag{54}$$

with $(\kappa\lambda)$ designating a transposition of indices κ and λ, and

$$\mathscr{S}^{\kappa\lambda} \equiv \mathscr{S}_{\kappa\lambda} = \mathscr{S}^{\kappa\lambda}(0) = \mathscr{S}_{\kappa\lambda}(0) = 1 + (\kappa\lambda). \tag{55}$$

To get the contribution corresponding to $\tilde{B}^{(1)}_{12}[G^{\alpha\beta}_{\varrho\sigma}(i)]$, we have to multiply the expression (53) by g^{kk}_{ll}. Now, if we use Eq. (48), with $\tilde{T}_2^{(1)}$ defined by Eq. (43), we must again consider four Hugenholtz diagrams. Brandow version of the diagram corresponding to the contribution (53) is shown in Fig. 4. As usual [11], the vertex representing the bra excitation operator $G^{\alpha\beta}_{\varrho\sigma}(i)$ is not explicitly shown. Instead, external lines carry the fixed orbital labels characterizing $G^{\alpha\beta}_{\varrho\sigma}(i)$, and different labelings of external lines are represented by the symmetrizer $\mathscr{S}^{\alpha\beta}$. As pointed out in [16, 17], this notation is very convenient, since it provides a one-to-one correspondence between the symmetrizers $\mathscr{S}^{\alpha\beta}$ ($\mathscr{S}_{\varrho\sigma}$) in orbital diagrams and the (anti)symmetrizers $\mathscr{S}^{\alpha\beta}(i)$ ($\mathscr{S}_{\varrho\sigma}(i)$) in algebraic expressions. As usual [16, 17], the summation over the intermediate spin quantum numbers S_i and S is already carried out in the diagram of Fig. 4. It can be easily verified that the spin diagram restricts the summation over S_i and S to only one term labeled by $S_i = S = i$. The algebraic expression corresponding to the diagram of Fig. 4 is thus:

$$2^{-\frac{3}{2}}[i]^{-\frac{1}{2}}N^{\alpha\beta}_{\varrho\sigma}\gamma^{k'k''}_{\varrho\sigma}(i)\,\mathscr{S}^{\alpha\beta}(i)\,{}^{(1)}t^{\alpha\,(2)}_{l'}t^{\beta l'}_{k''k'}(i). \tag{56}$$

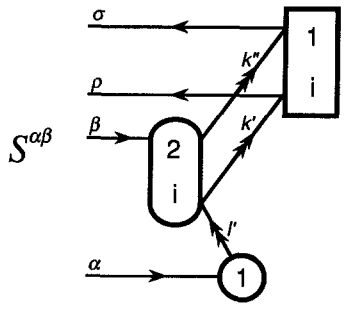

Fig. 4. Brandow-type orbital diagram yielding the contribution (53), when Eq. (48) with $\tilde{T}_2^{(1)}$ given by Eq. (43) is used (cf. Fig. 12a). The rightmost rectangular vertex serves as a graphical representation of $\tilde{T}_2^{(1)}$ (see Sect. 2 for details)

In this case, the spin diagram gives the factor $2^{-\frac{1}{2}}[i]^{-\frac{1}{2}}$, the bra state gives the normalization factor $N_{\varrho\sigma}^{\alpha\beta}$, and the weight is $\frac{1}{2}$. From the definition of the scalar factor $\gamma_{l'l''}^{k'k''}$, Eq. (44), it follows that

$$\gamma_{\varrho\sigma}^{k'k''}(i) = 2\delta_k^{k'}\delta_k^{k''}\delta_\varrho^l\delta_\sigma^l\delta_{i0}g_{ll}^{kk}, \tag{57}$$

so that we can rewrite Eq. (56) as

$$\begin{aligned} &2^{-\frac{1}{2}}\delta_{i0}[i]^{-\frac{1}{2}}N_{\varrho\sigma}^{\alpha\beta}\delta_k^{k'}\delta_k^{k''}\delta_\varrho^l\delta_\sigma^l g_{ll}^{kk}\mathscr{S}^{\alpha\beta}(i)\,{}^{(1)}t_{l'}^{\alpha}\,{}^{(2)}t_{k''k'}^{\beta l'}(i) \\ &\quad = 2^{-\frac{1}{2}}\delta_{i0}N_{\varrho\sigma}^{\alpha\beta}\delta_\varrho^l\delta_\sigma^l g_{ll}^{kk}\mathscr{S}^{\alpha\beta}\,{}^{(1)}t_{l'}^{\alpha}\,{}^{(2)}t_{kk}^{\beta l'}(0), \end{aligned} \tag{58}$$

where the summation over l' extends over one value, namely $l' = l$. This is precisely the previous result, Eq. (53). We thus see that both the calculation of the matrix element B, Eq. (52), and the application of Eq. (48) with $\tilde{T}_2^{(1)}$ defined by Eq. (43), lead to the same result. The latter method requires the presence of the $\tilde{T}_2^{(1)}$ vertex in the orbital diagram that can be avoided when the former approach is used. Moreover, calculation of slightly more general matrix elements between $\langle {}^{(1)}G_\alpha^\varrho\Phi_1|$ or $\langle {}^{(1)}G_{\alpha\beta}^{\varrho\sigma}(i)\Phi_1|$ and $|{}^{(1)}G_{k\bar{k}}^{l\bar{l}}(S)\Phi_1\rangle$ may be useful, when more than two active orbitals are involved. Although this increased generality can also be achieved by redefining $\gamma_{l'l''}^{k'k''}(S)$, in the following we employ the method, which is based on the evaluation of the matrix elements between $\langle {}^{(1)}G_i\Phi_1|$ and $|{}^{(1)}G_{k\bar{k}}^{l\bar{l}}(S)\Phi_1\rangle$.

3.1. Explicit expressions for linear terms

Consider, first, the linear terms $R_n^{(1)}(G_l^\dagger)$ $(n = 1, 2)$. It can be verified (cf. the discussion before Eq. (35)) that

$$\langle\Phi_1|{}^{(1)}G_\varrho^\alpha T_1^{(2)}\,{}^{(1)}G_{k\bar{k}}^{l\bar{l}}(S)|\Phi_1\rangle = 0, \tag{59}$$

so that, in particular,

$$R_1^{(1)}(G_\varrho^\alpha) = 0. \tag{60}$$

For the two-body component, $R_1^{(1)}[G_{\varrho\sigma}^{\alpha\beta}(i)]$, we can draw two distinct Hugenholtz diagrams that correspond to a single nonoriented Hugenholtz skeleton shown in Fig. 5. Their Brandow representatives, associated with the general matrix element $\langle\Phi_1|{}^{(1)}G_{\varrho\sigma}^{\alpha\beta}(i)T_1^{(2)}\,{}^{(1)}G_{k\bar{k}}^{l\bar{l}}(S)|\Phi_1\rangle$, are given in Fig. 5a,b. Notice that Brandow vertices representing ${}^{(1)}G_{\varrho\sigma}^{\alpha\beta}(i)$ and ${}^{(1)}G_{k\bar{k}}^{l\bar{l}}(S)$, Fig. 2g and 2i, respectively, are not explicitly shown. Instead, as in the diagram of Fig. 4, all external lines are labeled by the fixed orbital indices characterizing the operators ${}^{(1)}G_{\varrho\sigma}^{\alpha\beta}(i)$ and

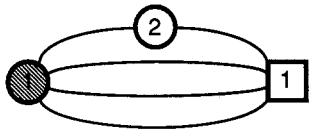

Fig. 5. Nonoriented Hugenholtz skeleton corresponding to $R_1^{(1)}[G_{\varrho\sigma}^{\alpha\beta}(i)]$

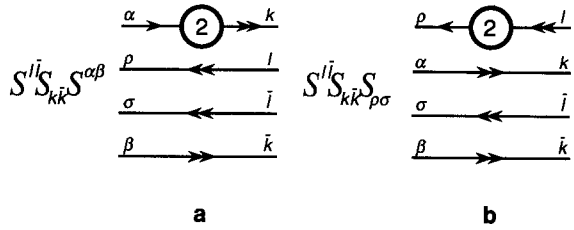

Fig. 5a,b. Brandow diagrams corresponding to $\langle\Phi_1|{}^{(1)}G_{\varrho\sigma}^{\alpha\beta}(i)T_1^{(2)}\,{}^{(1)}G_{k\bar{k}}^{ll}(S)|\Phi_1\rangle$, representing the successive terms on the right-hand side of Eq. (61)

${}^{(1)}G_{k\bar{k}}^{ll}(S)$, and distinct labeling schemes carried by the external lines are represented by the symmetrizers $\mathscr{S}^{\alpha\beta}$, $\mathscr{S}_{\varrho\sigma}$, $\mathscr{S}^{ll}$ and $\mathscr{S}_{k\bar{k}}$ (see [17]). In this way, the resulting diagrams (Fig. 5a,b) are much more transparent than in the case when all the vertices are explicitly shown. However, in determining the sign factor $(-1)^{l+h}$, where l designates the number of closed loops and h the number of internal hole lines (cf. [14]), we have to join all the external lines of our diagrams (cf. Fig. 5a,b) with vertices representing the excitation operators, ${}^{(1)}G_{\varrho\sigma}^{\alpha\beta}(i)$ on the left and ${}^{(1)}G_{k\bar{k}}^{ll}(S)$ on the right [cf. Fig. 2g and 2i, respectively], and regard them as internal lines.

To obtain the final algebraic expression that is associated with a given diagram, we evaluate and combine orbital and spin factors corresponding to each diagram while ignoring the symmetrizers, and replace the symmetrizers $\mathscr{S}^{\alpha\beta}$, $\mathscr{S}_{\varrho\sigma}$, $\mathscr{S}^{ll}$ and $\mathscr{S}_{k\bar{k}}$ with operators $\mathscr{S}^{\alpha\beta}(i)$, $\mathscr{S}_{\varrho\sigma}(i)$, $\mathscr{S}^{ll}(S)$ and $\mathscr{S}_{k\bar{k}}(S)$, respectively [16, 17]. Spin diagrams and the pertinent orbital and spin factors are listed in the Appendix.

Evaluation of diagrams 5a and 5b thus gives:

$$\langle\Phi_1|{}^{(1)}G_{\varrho\sigma}^{\alpha\beta}(i)T_1^{(2)}\,{}^{(1)}G_{k\bar{k}}^{ll}(S)|\Phi_1\rangle = -2^{-\frac{1}{2}}\delta_{iS}N_{\varrho\sigma}^{\alpha\beta}N_{k\bar{k}}^{ll}\mathscr{S}^{ll}(S)\mathscr{S}_{k\bar{k}}(S)[\delta_\varrho^l\delta_\sigma^{\bar{l}}\mathscr{S}^{\alpha\beta}(S)\,{}^{(2)}t_k^\alpha\delta_{\bar{k}}^\beta - \delta_k^\alpha\delta_{\bar{k}}^\beta\mathscr{S}_{\varrho\sigma}(S)\,{}^{(2)}t_\varrho^l\delta_\sigma^{\bar{l}}]. \tag{61}$$

To obtain the expression for $R_1^{(1)}[G_{\varrho\sigma}^{\alpha\beta}(i)]$, we assume that $k=\bar{k}$, $l=\bar{l}$, $S=0$, and multiply the result by g_{ll}^{kk}. Notice that the presence of $N_{k\bar{k}}^{ll}$ introduces the factor $\frac{1}{2}$, $S^{ll}(S)$ can be replaced by 2, and $\mathscr{S}_{k\bar{k}}(S)$ in Eq. (61) gives another factor of 2. As a result, we get

$$R_1^{(1)}[G_{\varrho\sigma}^{\alpha\beta}(i)] = -2^{\frac{1}{2}}\delta_{i0}g_{ll}^{kk}N_{\varrho\sigma}^{\alpha\beta}[\delta_\varrho^l\delta_\sigma^l\mathscr{S}^{\alpha\beta}\,{}^{(2)}t_k^\alpha\delta_k^\beta - \delta_k^\alpha\delta_k^\beta\mathscr{S}_{\varrho\sigma}\,{}^{(2)}t_\varrho^l\delta_\sigma^l], \tag{62}$$

or, in fact,

$$R_1^{(1)}[G_{\varrho\sigma}^{\alpha\beta}(i)] = -\delta_{i0}g_{ll}^{kk}[\delta_\varrho^l\delta_\sigma^l\mathscr{S}^{\alpha\beta}\,{}^{(2)}t_k^\alpha\delta_k^\beta - \delta_k^\alpha\delta_k^\beta\mathscr{S}_{\varrho\sigma}\,{}^{(2)}t_\varrho^l\delta_\sigma^l]. \tag{62'}$$

To derive Eq. (62'), we observe that in order to get a nonzero result, we must have either $\varrho=\sigma=l$, $\alpha\neq\beta$ (α or $\beta=k$) or $\alpha=\beta=k$, $\varrho\neq\sigma$ (ϱ or $\sigma=l$), so that always $N_{\varrho\sigma}^{\alpha\beta}=2^{-\frac{1}{2}}$ [cf. Eq. (2')], since α and ϱ in ${}^{(2)}t_\varrho^\alpha$ cannot simultaneously be valence labels.

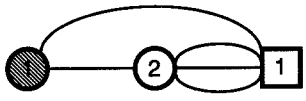

Fig. 6. Nonoriented Hugenholtz skeleton corresponding to $R_2^{(1)}(G_\varrho^\alpha)$

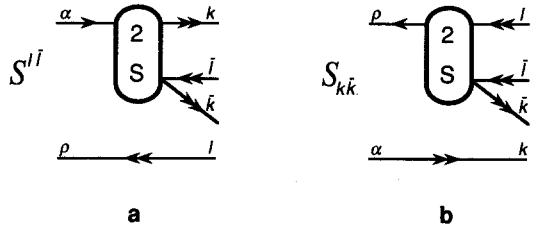

Fig. 6a,b. Brandow diagrams corresponding to $\langle \Phi_1 | {}^{(1)}G_\varrho^\alpha T_2^{(2)}\, {}^{(1)}G_{k\bar{k}}^{ll}(S) | \Phi_1 \rangle$. They represent successive terms on the right-hand side of Eq. (63)

We next consider the linear term $R_2^{(1)}(G_i^\dagger)$. For the one-body component $R_2^{(1)}(G_\varrho^\alpha)$ we get two Hugenholtz diagrams that correspond to a single nonoriented Hugenholtz skeleton of Fig. 6. The corresponding Brandow diagrams for the matrix element $\langle \Phi_1 | {}^{(1)}G_\varrho^\alpha T_2^{(2)}\, {}^{(1)}G_{k\bar{k}}^{ll}(S) | \Phi_1 \rangle$ are shown in Fig. 6a,b. Evaluating these diagrams and corresponding spin graphs (cf. Appendix), we get

$$\langle \Phi_1 | {}^{(1)}G_\varrho^\alpha T_2^{(2)}\, {}^{(1)}G_{k\bar{k}}^{ll}(S) | \Phi_1 \rangle = -2^{-\frac{1}{2}} N_{k\bar{k}}^{ll} [\mathscr{S}^{ll}(S)\, {}^{(2)}t_{k\bar{k}}^{\alpha l}(S)\delta_\varrho^l - \mathscr{S}_{k\bar{k}}(S)\, {}^{(2)}t_{\varrho\bar{k}}^{ll}(S)\delta_k^\alpha], \tag{63}$$

so that the expression for

$$R_2^{(1)}(G_\varrho^\alpha) = g_{ll}^{kk} \langle \Phi_1 | {}^{(1)}G_\varrho^\alpha T_2^{(2)} G_{kk}^{ll}(0) | \Phi_1 \rangle \tag{64}$$

is

$$R_2^{(1)}(G_\varrho^\alpha) = -2^{-\frac{1}{2}} g_{ll}^{kk} [{}^{(2)}t_{kk}^{\alpha l}(0)\delta_\varrho^l - {}^{(2)}t_{\varrho k}^{ll}(0)\delta_k^\alpha]. \tag{65}$$

The only nonvanishing cases are $R_2^{(1)}(G_l^a)$ and $R_2^{(1)}(G_r^k)$.

For the two-body part $R_2^{(1)}[G_{\varrho\sigma}^{\alpha\beta}(i)]$, we can also draw a single nonoriented Hugenholtz skeleton (Fig. 7). The corresponding Brandow diagrams that are associated with the matrix element $\langle \Phi_1 | {}^{(1)}G_{\varrho\sigma}^{\alpha\beta}(i) T_2^{(2)}\, {}^{(1)}G_{k\bar{k}}^{ll}(S) | \Phi_1 \rangle$ are given in

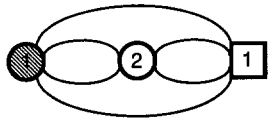

Fig. 7. Nonoriented Hugenholtz skeleton corresponding to $R_2^{(1)}[G_{\varrho\sigma}^{\alpha\beta}(i)]$

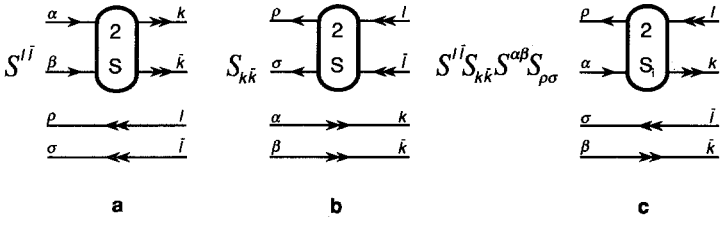

Fig. 7a–c. Brandow diagrams corresponding to $\langle \Phi_1 | {}^{(1)}G_{\varrho\sigma}^{\alpha\beta}(i) T_2^{(2)}\, {}^{(1)}G_{k\bar{k}}^{ll}(S) | \Phi_1 \rangle$. They are associated with successive terms on the right-hand side of Eq. (66)

Fig. 7a–c. Notice that spin coupling coefficients corresponding to *hh* and *pp* cases [diagrams 7a and 7b] restrict the summation over S_i to only one term, $S_i = S$, while for the *ph* case [diagram 7c], the summation over the intermediate spin quantum number ($S_i = 0$ and 1) remains. Evaluation of diagrams 7a–c yields:

$$\langle \Phi_1 | {}^{(1)}G^{\alpha\beta}_{\varrho\sigma}(i) T_2^{(2)\,(1)} G^{lI}_{k\bar{k}}(S) | \Phi_1 \rangle$$

$$= N^{\alpha\beta}_{\varrho\sigma} N^{lI}_{k\bar{k}} \left\{ \delta_{iS}[S]^{-\frac{1}{2}} ({}^{(2)}t^{\alpha\beta}_{k\bar{k}}(S) \mathscr{S}^{lI}(S) \delta^{l}_{\varrho} \delta^{I}_{\sigma} + {}^{(2)}t^{lI}_{\varrho\sigma}(S) \mathscr{S}_{k\bar{k}}(S) \delta^{\alpha}_{k} \delta^{\beta}_{\bar{k}}) \right.$$

$$\left. + \mathscr{S}^{lI}(S) \mathscr{S}_{k\bar{k}}(S) \mathscr{S}^{\alpha\beta}(i) \mathscr{S}_{\varrho\sigma}(i) \delta^{I}_{\sigma} \delta^{\beta}_{k} \sum_{S_i=0}^{1} [i, S_i, S]^{\frac{1}{2}} C(i, S_i, S)\, {}^{(2)}t^{\alpha l}_{\varrho k}(S_i) \right\}, \quad (66)$$

where the multiple symbol $[X_1, X_2, \ldots, X_n]$ designates the product $\prod_{k=1}^{n} [X_k]$ and C is a well-known (cf. [11]) 9-*j* coefficient

$$C(X_1, X_2, X_3) = \begin{Bmatrix} X_1 & \frac{1}{2} & \frac{1}{2} \\ \frac{1}{2} & X_2 & \frac{1}{2} \\ \frac{1}{2} & \frac{1}{2} & X_3 \end{Bmatrix}. \quad (67)$$

Assuming $k = \bar{k}$, $l = \bar{l}$, $S = 0$, multiplying the resulting expression by g^{kk}_{ll}, and using the relation

$$C(X_1, X_2, 0) = \tfrac{1}{2} U(X_1, X_2), \quad (68)$$

where U is the 6-*j* coefficient defined by

$$U(X_1, X_2) = U(X_2, X_1) = \begin{Bmatrix} \frac{1}{2} & \frac{1}{2} & X_1 \\ \frac{1}{2} & \frac{1}{2} & X_2 \end{Bmatrix}, \quad (69)$$

we find that

$$R_2^{(1)}[G^{\alpha\beta}_{\varrho\sigma}(i)] = g^{kk}_{ll} N^{\alpha\beta}_{\varrho\sigma} \left\{ \delta_{i0} [{}^{(2)}t^{\alpha\beta}_{kk}(0) \delta^{l}_{\varrho} \delta^{l}_{\sigma} + {}^{(2)}t^{ll}_{\varrho\sigma}(0) \delta^{\alpha}_{k} \delta^{\beta}_{k}] \right.$$

$$\left. + \mathscr{S}^{\alpha\beta}(i) \mathscr{S}_{\varrho\sigma}(i) \delta^{l}_{\sigma} \delta^{\beta}_{k} \sum_{S_i=0}^{1} [i, S_i]^{\frac{1}{2}} U(i, S_i)\, {}^{(2)}t^{\alpha l}_{\varrho k}(S_i) \right\}. \quad (70)$$

The first term in Eq. (70) contributes only when $\alpha = a$, $\beta = b$, $\varrho = \sigma = l$, the second one contributes when $\alpha = \beta = k$, $\varrho = r$, $\sigma = s$, while the third term becomes nonzero only when the operator ${}^{(1)}G^{\alpha\beta}_{\varrho\sigma}(i)$ is of the type $G^{ak}_{rl}(i)$. Otherwise, $R_2^{(1)}[G^{\alpha\beta}_{\varrho\sigma}(i)]$ vanishes.

3.2. Explicit expressions for bilinear terms

Here we have to consider four distinct contributions, namely, $B^{(1)}_{nn}(G^{\dagger}_{l})$ ($n = 1, 2$), $B^{(1)}_{12}(G^{\dagger}_{l})$, and $\tilde{B}^{(1)}_{12}(G^{\dagger}_{l})$. Although the latter two contributions can be replaced by the single term $\tilde{\tilde{B}}^{(1)}_{12}(G^{\dagger}_{l})$, Eq. (41), in this section we examine them separately, since we wish to compare our results with those of [3]. Direct evaluation of the contribution $\tilde{\tilde{B}}^{(1)}_{12}(G^{\dagger}_{l})$ is discussed in the next section.

Since no vacuum diagrams can be drawn for $B^{(1)}_{11}(G^{\alpha}_{\varrho})$ (all the lines on the leftmost $T_1^{(2)}$ vertex would extend to the right), we have that

$$\tfrac{1}{2} \langle \Phi_1 | {}^{(1)}G^{\alpha}_{\varrho} T_1^{(2)2\,(1)} G^{lI}_{k\bar{k}}(S) | \Phi_1 \rangle = 0, \quad (71)$$

and

$$B^{(1)}_{11}(G^{\alpha}_{\varrho}) = 0. \quad (72)$$

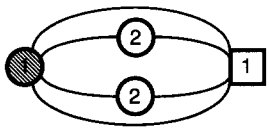

Fig. 8. Nonoriented Hugenholtz skeleton corresponding to $B_{11}^{(1)}[G_{\varrho\sigma}^{\alpha\beta}(i)]$

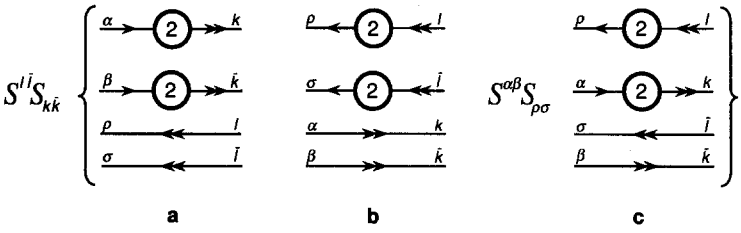

Fig. 8a–c. Brandow diagrams corresponding to $\frac{1}{2}\langle\Phi_1|{}^{(1)}G_{\varrho\sigma}^{\alpha\beta}(i)T_1^{(2)^2}\,{}^{(1)}G_{k\bar{k}}^{l\bar{l}}(S)|\Phi_1\rangle$. They are associated with successive terms on the right-hand side of Eq. (73)

However, for the two-body component $B_{11}^{(1)}[G_{\varrho\sigma}^{\alpha\beta}(i)]$ we can draw a nonoriented Hugenholtz skeleton shown in Fig. 8. The corresponding Brandow diagrams, representing the matrix element $\frac{1}{2}\langle\Phi_1|{}^{(1)}G_{\varrho\sigma}^{\alpha\beta}(i)T_1^{(2)^2}\,{}^{(1)}G_{k\bar{k}}^{l\bar{l}}(S)|\Phi_1\rangle$, are listed in Fig. 8a–c, and give:

$$\begin{aligned}\tfrac{1}{2}\langle\Phi_1|{}^{(1)}G_{\varrho\sigma}^{\alpha\beta}(i)T_1^{(2)^2}\,{}^{(1)}G_{k\bar{k}}^{l\bar{l}}(S)|\Phi_1\rangle &= \tfrac{1}{2}\delta_{iS}N_{\varrho\sigma}^{\alpha\beta}N_{k\bar{k}}^{l\bar{l}}\mathscr{S}^{l\bar{l}}(S)\mathscr{S}_{k\bar{k}}(S)\\ &\quad\times[{}^{(2)}t_k^{\alpha}\,{}^{(2)}t_{\bar{k}}^{\beta}\delta_{\varrho}^{l}\delta_{\sigma}^{\bar{l}}+{}^{(2)}t_{\varrho}^{l}\,{}^{(2)}t_{\sigma}^{\bar{l}}\delta_k^{\alpha}\delta_{\bar{k}}^{\beta}\\ &\quad-\mathscr{S}^{\alpha\beta}(S)\mathscr{S}_{\varrho\sigma}(S)\,{}^{(2)}t_k^{\alpha}\,{}^{(2)}t_{\varrho}^{l}\delta_{\bar{k}}^{\beta}\delta_{\sigma}^{\bar{l}}].\end{aligned}\tag{73}$$

Thus, the result for

$$B_{11}^{(1)}[G_{\varrho\sigma}^{\alpha\beta}(i)]=\tfrac{1}{2}g_{ll}^{kk}\langle\Phi_1|{}^{(1)}G_{\varrho\sigma}^{\alpha\beta}(i)T_1^{(2)^2}G_{kk}^{ll}(0)|\Phi_1\rangle\tag{74}$$

takes the following form:

$$B_{11}^{(1)}[G_{\varrho\sigma}^{\alpha\beta}(i)]=\delta_{i0}g_{ll}^{kk}N_{\varrho\sigma}^{\alpha\beta}[{}^{(2)}t_k^{\alpha}\,{}^{(2)}t_{\bar{k}}^{\beta}\delta_{\varrho}^{l}\delta_{\sigma}^{\bar{l}}+{}^{(2)}t_{\varrho}^{l}\,{}^{(2)}t_{\sigma}^{\bar{l}}\delta_k^{\alpha}\delta_{\bar{k}}^{\beta}-\mathscr{S}^{\alpha\beta}\mathscr{S}_{\varrho\sigma}\,{}^{(2)}t_k^{\alpha}\,{}^{(2)}t_{\varrho}^{l}\delta_{\bar{k}}^{\beta}\delta_{\sigma}^{\bar{l}}].\tag{75}$$

As in the case of $R_2^{(1)}[G_{\varrho\sigma}^{\alpha\beta}(i)]$, the first term in Eq. (75) contributes when $\alpha=a$, $\beta=b$, $\varrho=\sigma=l$, the second one becomes nonzero when $\alpha=\beta=k$, $\varrho=r$, $\sigma=s$, and the third one contributes only when ${}^{(1)}G_{\varrho\sigma}^{\alpha\beta}(i)$ is of the type $G_{rl}^{ak}(i)$. It is thus not surprising that $R_2^{(1)}[G_{\varrho\sigma}^{\alpha\beta}(i)]$ and $B_{11}^{(1)}[G_{\varrho\sigma}^{\alpha\beta}(i)]$ can be combined together assuming that the same expression is used for g_{ll}^{kk} entering Eqs. (70) and (75). This is certainly the case when all the nonlinear terms are taken into account in calculating the effective Hamiltonian. Using the explicit values of the 6-j coefficient $U(X_1, X_2)$, Eq. (69), (see Table 1), we can write:

$$\begin{aligned}&R_2^{(1)}[G_{\varrho\sigma}^{\alpha\beta}(i)]+B_{11}^{(1)}[G_{\varrho\sigma}^{\alpha\beta}(i)]\\ &\quad=g_{ll}^{kk}N_{\varrho\sigma}^{\alpha\beta}\{\delta_{i0}[\delta_{\varrho}^{l}\delta_{\sigma}^{\bar{l}}\,{}^{(2)}D_{kk}^{\alpha\beta}(0)+\delta_k^{\alpha}\delta_{\bar{k}}^{\beta}\,{}^{(2)}D_{\varrho\sigma}^{ll}(0)-\mathscr{S}^{\alpha\beta}\mathscr{S}_{\varrho\sigma}\delta_{\sigma}^{\bar{l}}\delta_{\bar{k}}^{\beta}\,{}^{(2)}M_{k\varrho}^{\alpha l}]\\ &\qquad+(1-\delta_{i0})\mathscr{S}^{\alpha\beta}(i)\mathscr{S}_{\varrho\sigma}(i)\delta_{\sigma}^{\bar{l}}\delta_{\bar{k}}^{\beta}\,{}^{(2)}P_{k\varrho}^{\alpha l}\},\end{aligned}\tag{76}$$

Table 1. Explicit values of 6-j coefficient $U(X_1, X_2)$, Eq. (69)

X_1	X_2	$U(X_1, X_2)$
0	0	$-\frac{1}{2}$
0	1	$\frac{1}{2}$
1	1	$\frac{1}{6}$

where

$$ {}^{(p)}D^{\alpha\beta}_{\varrho\sigma}(i) = {}^{(p)}t^{\alpha\beta}_{\varrho\sigma}(i) + \tfrac{1}{2}[i]^{\frac{1}{2}}\mathscr{S}^{\alpha\beta}(i)\,{}^{(p)}t^{\alpha}_{\varrho}\,{}^{(p)}t^{\beta}_{\sigma}, \tag{77} $$

$$ {}^{(p)}M^{\alpha\beta}_{\varrho\sigma} = {}^{(p)}A^{\alpha\beta}_{\varrho\sigma} + {}^{(p)}t^{\alpha}_{\varrho}\,{}^{(p)}t^{\beta}_{\sigma}, \tag{78} $$

$$ {}^{(p)}P^{\alpha\beta}_{\varrho\sigma} = \tfrac{1}{2}[3^{\frac{1}{2}}\,{}^{(p)}t^{\alpha\beta}_{\varrho\sigma}(0) - {}^{(p)}t^{\alpha\beta}_{\varrho\sigma}(1)], \tag{79} $$

and

$$ {}^{(p)}A^{\alpha\beta}_{\varrho\sigma} = \tfrac{1}{2}[{}^{(p)}t^{\alpha\beta}_{\varrho\sigma}(0) + 3^{\frac{1}{2}}\,{}^{(p)}t^{\alpha\beta}_{\varrho\sigma}(1)]. \tag{80} $$

Notice that the expressions ${}^{(p)}D^{\alpha\beta}_{\varrho\sigma}(i)$, Eq. (77), and ${}^{(p)}A^{\alpha\beta}_{\varrho\sigma}$, Eq. (80), appear in the SR orthogonally spin-adapted CCSD equations [16]. The quantity ${}^{(p)}M^{\alpha\beta}_{\varrho\sigma}$ can also be written as

$$ {}^{(p)}M^{\alpha\beta}_{\varrho\sigma} = \tfrac{1}{2}[{}^{(p)}E^{\beta\alpha}_{\varrho\sigma}(0) - 3^{\frac{1}{2}}\,{}^{(p)}E^{\beta\alpha}_{\varrho\sigma}(1)], \tag{81} $$

where

$$ {}^{(p)}E^{\alpha\beta}_{\varrho\sigma}(i) = {}^{(p)}t^{\alpha\beta}_{\varrho\sigma}(i) + \tfrac{1}{2}(-1)^{i}[i]^{\frac{1}{2}}\,{}^{(p)}t^{\beta}_{\varrho}\,{}^{(p)}t^{\alpha}_{\sigma}, \tag{82} $$

which is another expression that appears in the direct term [16]. Clearly, this is not a coincidence. Indeed, quantities ${}^{(p)}A^{\alpha\beta}_{\varrho\sigma}$, ${}^{(p)}D^{\alpha\beta}_{\varrho\sigma}(i)$, ${}^{(p)}E^{\alpha\beta}_{\varrho\sigma}(i)$, etc. enter the direct term when we group together the connected and disconnected cluster components of the same excitation order, which is the case in Eq. (76), where we grouped $T_2^{(2)}$ with $\frac{1}{2}T_1^{(2)^2}$. In diagrammatic language, we can say that the term $\frac{1}{2}T_1^{(2)^2}$ results from a "splitting" of the $T_2^{(2)}$ vertex into the two $T_1^{(2)}$ vertices (cf. Fig. 8a–c with Fig. 7a–c and the discussion in [16]). No such splitting is possible when we consider the one-body component $R_2^{(1)}(G^{\alpha}_{\varrho})$, since one of the $T_1^{(2)}$ vertices in the resulting diagram would carry only the valence labels (see Fig. 6a,b). Consequently, $B_{11}^{(1)}(G^{\alpha}_{\varrho}) = 0$ (cf. Eq. (72)).

Consider, next, the nonlinear term $B_{22}^{(1)}(G_i^{\dagger})$. For the one-body component $B_{22}^{(1)}(G^{\alpha}_{\varrho})$, no vacuum diagrams can be formed, so that

$$ \tfrac{1}{2}\langle\Phi_1|{}^{(1)}G^{\alpha}_{\varrho}T_2^{(2)^2}\,{}^{(1)}G^{\mathit{ll}}_{k\bar{k}}(S)|\Phi_1\rangle = 0, \tag{83} $$

and

$$ B_{22}^{(1)}(G^{\alpha}_{\varrho}) = 0. \tag{84} $$

For the two-body part $B_{22}^{(1)}[G^{\alpha\beta}_{\varrho\sigma}(i)]$, we can construct two nonoriented Hugenholtz skeletons (Fig. 9) of four Brandow diagrams (Fig. 9a–d). As in the preceding cases, the Brandow diagrams (Fig. 9a–d) correspond to a general matrix element $\frac{1}{2}\langle\Phi_1|{}^{(1)}G^{\alpha\beta}_{\varrho\sigma}(i)T_2^{(2)^2}\,{}^{(1)}G^{\mathit{ll}}_{k\bar{k}}(S)|\Phi_1\rangle$. Combining the orbital and spin

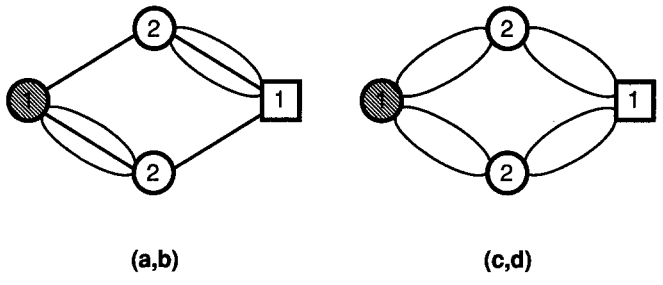

Fig. 9. Nonoriented Hugenholtz skeletons corresponding to $B^{(1)}_{22}[G^{\alpha\beta}_{\varrho\sigma}(i)]$. (x, y) indicates which Brandow diagrams of Fig. 9a–d are associated with a given skeleton

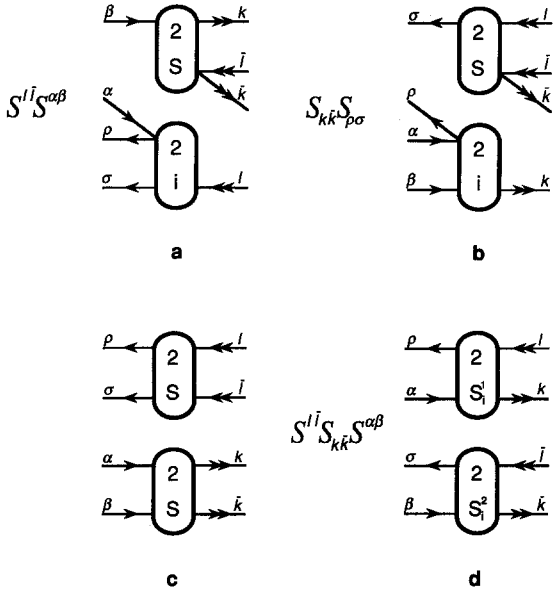

Fig. 9a–d. Brandow diagrams corresponding to $\frac{1}{2}\langle\Phi_1|{}^{(1)}G^{\alpha\beta}_{\varrho\sigma}(i)T^{(2)^2}_2\,{}^{(1)}G^{l\bar{l}}_{k\bar{k}}(S)|\Phi_1\rangle$. They are associated with successive terms on the right-hand side of Eq. (85)

factors (cf. Appendix) gives:

$$\begin{aligned}\tfrac{1}{2}\langle\Phi_1|{}^{(1)}G^{\alpha\beta}_{\varrho\sigma}(i)T^{(2)^2}_2\,{}^{(1)}G^{l\bar{l}}_{k\bar{k}}(S)|\Phi_1\rangle = N^{\alpha\beta}_{\varrho\sigma}N^{l\bar{l}}_{k\bar{k}}\Big\{&-\tfrac{1}{2}[\mathscr{S}^{l\bar{l}}(S)\mathscr{S}^{\alpha\beta}(i)\,{}^{(2)}t^{\alpha l}_{\varrho\sigma}(i)\,{}^{(2)}t^{\beta\bar{l}}_{k\bar{k}}(S)\\ &+\mathscr{S}_{k\bar{k}}(S)\mathscr{S}_{\varrho\sigma}(i)\,{}^{(2)}t^{\alpha\beta}_{\varrho k}(i)\,{}^{(2)}t^{l\bar{l}}_{\sigma\bar{k}}(S)]+\delta_{iS}[S]^{-1}\,{}^{(2)}t^{\alpha\beta}_{k\bar{k}}(S)\,{}^{(2)}t^{l\bar{l}}_{\varrho\sigma}(S)\\ &+\sum_{S^1_iS^2_i}[i,S^1_i,S^2_i,S]^{\frac{1}{2}}R(i,S^1_i,S^2_i,S)\mathscr{S}^{l\bar{l}}(S)\mathscr{S}_{k\bar{k}}(S)\mathscr{S}^{\alpha\beta}(i)\,{}^{(2)}t^{\alpha l}_{\varrho k}(S^1_i)\,{}^{(2)}t^{\beta\bar{l}}_{\sigma\bar{k}}(S^2_i)\Big\},\end{aligned} \tag{85}$$

where the coefficient $R(X_1, X_2, X_3, X_4)$ is a 12-j symbol of the second kind [12] defined by (cf. [16, 17])

$$R(X_1,X_2,X_3,X_4)=\begin{bmatrix}\frac{1}{2} & \frac{1}{2} & \frac{1}{2} & \frac{1}{2}\\ X_1 & X_2 & X_3 & X_4\\ \frac{1}{2} & \frac{1}{2} & \frac{1}{2} & \frac{1}{2}\end{bmatrix}. \tag{86}$$

Assuming $k=\bar{k}$, $l=\bar{l}$, $S=0$, multiplying the resulting expression by g^{kk}_{ll}, and using the relation [12]

$$R(X_1,X_2,X_3,0)=\tfrac{1}{2}V(X_1,X_2,X_3)^2, \tag{87}$$

where V is the 6-j coefficient defined by

$$V(X_1, X_2, X_3) = \begin{Bmatrix} X_1 & X_2 & X_3 \\ \frac{1}{2} & \frac{1}{2} & \frac{1}{2} \end{Bmatrix}, \tag{88}$$

we obtain

$$B_{22}^{(1)}[G_{\varrho\sigma}^{\alpha\beta}(i)] = \tfrac{1}{2} g_{ll}^{kk} N_{\varrho\sigma}^{\alpha\beta} \Big\{ -\mathscr{S}^{\alpha\beta}(i)\, {}^{(2)}t_{\varrho\sigma}^{\alpha l}(i)\, {}^{(2)}t_{kk}^{\beta l}(0) - \mathscr{S}_{\varrho\sigma}(i)\, {}^{(2)}t_{\varrho k}^{\alpha\beta}(i)\, {}^{(2)}t_{\sigma k}^{ll}(0)$$
$$+ \delta_{i0}\, {}^{(2)}t_{kk}^{\alpha\beta}(0)\, {}^{(2)}t_{\varrho\sigma}^{ll}(0) + 2 \sum_{S_i^1 S_i^2} [i, S_i^1, S_i^2]^{\frac{1}{2}} V(i, S_i^1, S_i^2)^2$$
$$\times \mathscr{S}^{\alpha\beta}(i)\, {}^{(2)}t_{\varrho k}^{\alpha l}(S_i^1)\, {}^{(2)}t_{\sigma k}^{\beta l}(S_i^2) \Big\}. \tag{89}$$

The 6-j coefficient V, Eq. (88), has the same symmetry properties as the 9-j symbol C, Eq. (67), namely

$$V(X_1, X_2, X_3) = V(X_{i_1}, X_{i_2}, X_{i_3}), \tag{90}$$

for any permutation of indices 1, 2, 3. Equation (89) implies that $B_{22}^{(1)}[G_{\varrho\sigma}^{\alpha\beta}(i)] \neq 0$ only when α and β are core orbitals and ϱ and σ are virtual orbitals. This is also clear from Fig. 9a–d, since $T^{(2)}$ vertices cannot have valence lines to the left (cf. Fig. 3).

Let us now turn to the most complicated bilinear term, namely, $B_{12}^{(1)}(G_i^\dagger)$. For the one-body component $B_{12}^{(1)}(G_\varrho^\alpha)$ we can draw two Hugenholtz diagrams that follow from a single nonoriented Hugenholtz skeleton of Fig. 10. The corresponding Brandow diagrams, associated with the matrix element $\langle \Phi_1 | {}^{(1)}G_\varrho^\alpha T_2^{(2)}(T_1^{(2)} - T_1^{(1)})\, {}^{(1)}G_{kk}^{ll}(S) | \Phi_1 \rangle$, are shown in Fig. 10a,b. Notice that there is no contribution from the vacuum diagrams containing the $T_1^{(1)}$ vertex: In these diagrams, $T_2^{(2)}$ vertex would have to carry only valence labels. Thus, after evaluating the orbital and spin factors corresponding to diagrams 10a and 10b, we can write:

$$\langle \Phi_1 | {}^{(1)}G_\varrho^\alpha T_2^{(2)}(T_1^{(2)} - T_1^{(1)})\, {}^{(1)}G_{kk}^{ll}(S) | \Phi_1 \rangle = \langle \Phi_1 | {}^{(1)}G_\varrho^\alpha T_2^{(2)} T_1^{(2)}\, {}^{(1)}G_{kk}^{ll}(S) | \Phi_1 \rangle$$
$$= -\tfrac{1}{2} N_{kk}^{ll} [\mathscr{S}^{ll}(S)\, {}^{(2)}t_{kk}^{\alpha l}(S)\, {}^{(2)}t_\varrho^l + \mathscr{S}_{k\varrho}(S)\, {}^{(2)}t_{\varrho k}^{ll}(S)\, {}^{(2)}t_k^\alpha]. \tag{91}$$

Consequently, the result for

$$B_{12}^{(1)}(G_\varrho^\alpha) = g_{ll}^{kk} \langle \Phi_1 | {}^{(1)}G_\varrho^\alpha T_2^{(2)}(T_1^{(2)} - T_1^{(1)}) G_{kk}^{ll}(0) | \Phi_1 \rangle$$
$$= g_{ll}^{kk} \langle \Phi_1 | {}^{(1)}G_\varrho^\alpha T_2^{(2)} T_1^{(2)} G_{kk}^{ll}(0) | \Phi_1 \rangle \tag{92}$$

is

$$B_{12}^{(1)}(G_\varrho^\alpha) = -\tfrac{1}{2} g_{ll}^{kk} [{}^{(2)}t_{kk}^{\alpha l}(0)\, {}^{(2)}t_\varrho^l + {}^{(2)}t_{\varrho k}^{ll}(0)\, {}^{(2)}t_k^\alpha], \tag{93}$$

which means that $B_{12}^{(1)}(G_\varrho^\alpha) \neq 0$ only when α is core and ϱ is a virtual orbital label. This is again immediately obvious from Fig. 10a,b, since $T^{(2)}$ vertices cannot have valence lines extending to the left (cf. Fig. 3).

For the two-body component $B_{12}^{(1)}[G_{\varrho\sigma}^{\alpha\beta}(i)]$ we can draw as many as four distinct nonoriented Hugenholtz skeletons: two for the term involving $T_2^{(2)} T_1^{(2)}$ product, and another two for the term involving $T_2^{(2)} T_1^{(1)}$ product. They are

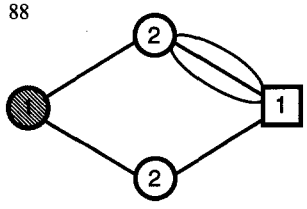

Fig. 10. Nonoriented Hugenholtz skeleton corresponding to $B^{(1)}_{12}(G^{\alpha}_{\varrho})$

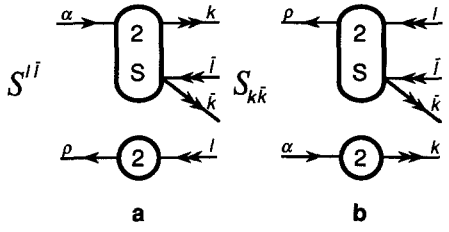

Fig. 10a,b. Brandow diagrams corresponding to $\langle\Phi_1|^{(1)}G^{\alpha}_{\varrho}T^{(2)}_2(T^{(2)}_1 - T^{(1)}_1)\,{}^{(1)}G^{l\bar{l}}_{k\bar{k}}(S)|\Phi_1\rangle = \langle\Phi_1|^{(1)}G^{\alpha}_{\varrho}T^{(2)}_2T^{(2)}_1\,{}^{(1)}G^{l\bar{l}}_{k\bar{k}}(S)|\Phi_1\rangle$. They represent two terms on the right-hand side of Eq. (91)

shown in Fig. 11. The corresponding Brandow diagrams, associated with the matrix element $\langle\Phi_1|^{(1)}G^{\alpha\beta}_{\varrho\sigma}(i)T^{(2)}_2(T^{(2)}_1 - T^{(1)}_1)\,{}^{(1)}G^{l\bar{l}}_{k\bar{k}}(S)|\Phi_1\rangle$, are given in Fig. 11a–h. Minus signs associated with the two triples of diagrams 11d and 11h indicate that the corresponding algebraic expressions have to be subtracted. Notice the presence of diagrams[1] $11d_2$, d_3, h_2 and h_3, in which the vertices $T^{(2)}_2$ and $T^{(1)}_1$ are connected. Obviously, contractions between $T^{(2)}_2$ and $T^{(1)}_1$ may only involve valence indices that distinguish Φ_1 and Φ_2. Formally, valence indices k' and l' are summation labels (k' occupied in $|\Phi_1\rangle$ and unoccupied in $|\Phi_2\rangle$, l' occupied in $|\Phi_2\rangle$ and unoccupied in $|\Phi_1\rangle$, which, in the final expressions, assume a single value, namely $k' = k$ and $l' = l$. Evaluation of the orbital and spin factors associated with diagrams 11a–h leads to the following

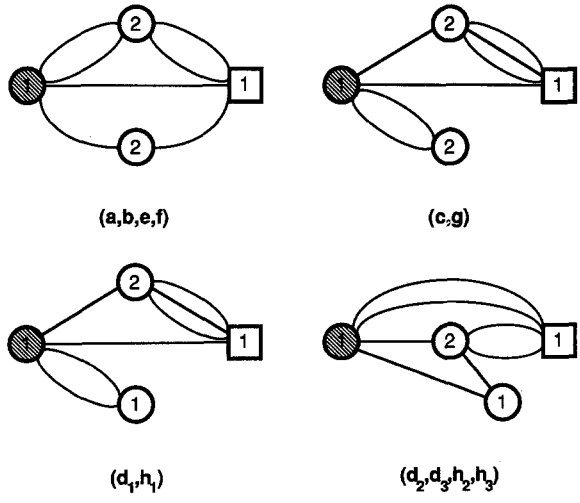

Fig. 11. Nonoriented Hugenholtz skeletons corresponding to $B^{(1)}_{12}[G^{\alpha\beta}_{\varrho\sigma}(i)]$. $(x, y, \ldots)$ indicates which Brandow diagrams of Fig. 11a–h are associated with a given skeleton. We must remember that expressions corresponding to diagrams obtained from skeletons (d_1, h_1) and (d_2, d_3, h_2, h_3) will have to be taken with the minus sign

[1] For simplicity, the ith diagram in Fig. Nx is designated as diagram Nx_i. Thus, for example, the rightmost diagram in Fig. 11d is referred to as diagram $11d_3$.

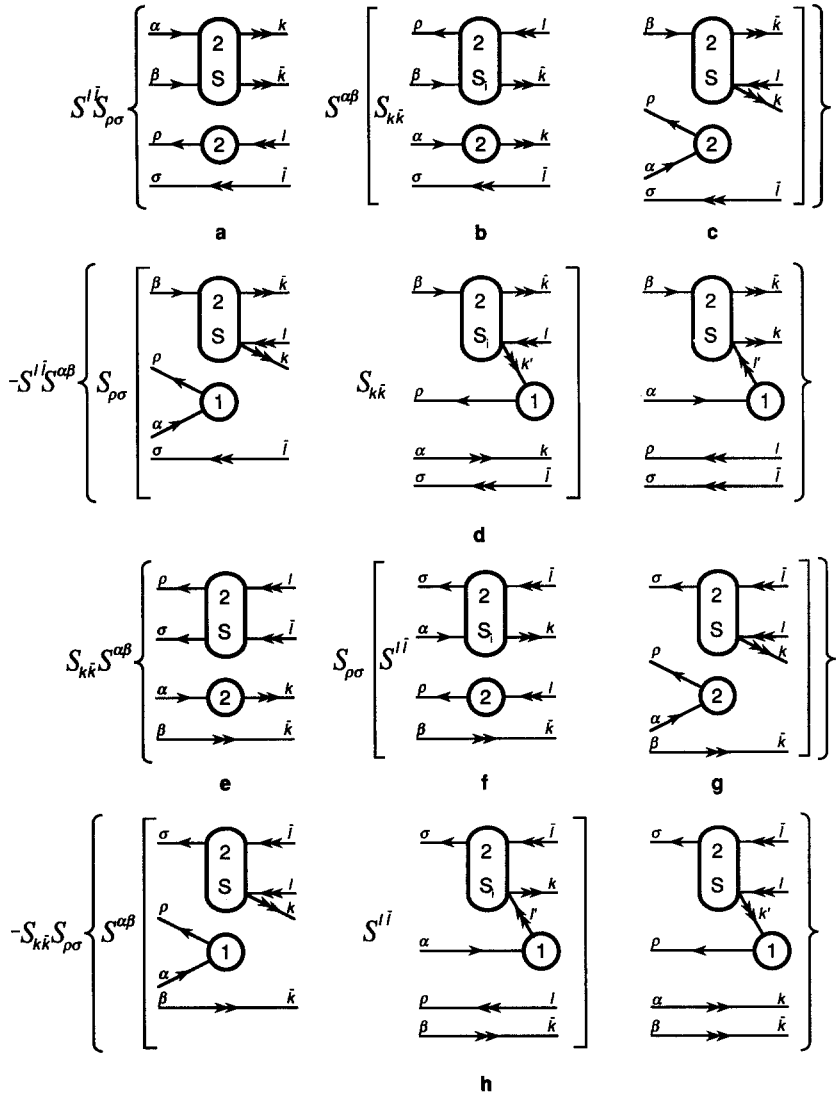

Fig. 11a–h. Brandow diagrams corresponding to $\langle\Phi_1|^{(1)}G^{\alpha\beta}_{\rho\sigma}(i)T_2^{(2)}(T_1^{(2)}-T_1^{(1)})^{(1)}G^{ij}_{k\bar{k}}(S)|\Phi_1\rangle$. They are associated with successive terms on the right-hand side of Eq. (94)

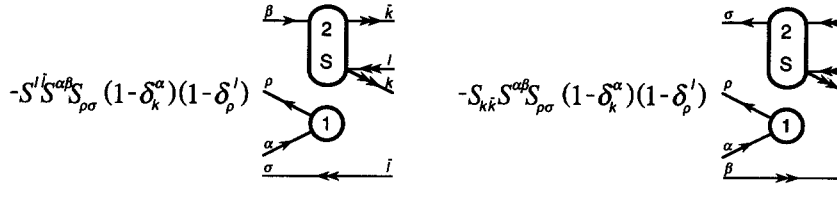

Fig. 11'd,h. Brandow diagrams which can be used instead of Figs. 11d and 11h when $k=\bar{k}=k'$, $l=\bar{l}=l'$ and $S=0$. They correspond to expressions (99) (diagram d) and (101) (diagram h), or to the fourth and eighth terms in Eq. (103)

expression:

$$\langle \Phi_1 |{}^{(1)}G^{\alpha\beta}_{\varrho\sigma}(i)T_2^{(2)}(T_1^{(2)} - T_1^{(1)})\,{}^{(1)}G^{II}_{k\bar{k}}(S)\,|\Phi_1\rangle$$

$$= 2^{-\frac{1}{2}}N^{\alpha\beta}_{\varrho\sigma}N^{II}_{k\bar{k}}\Bigg(\mathscr{S}^{II}(S)\Bigg\{\mathscr{S}_{\varrho\sigma}(i)\Bigg[\delta_{iS}[S]^{-\frac{1}{2}}\,{}^{(2)}t^{l}_{\varrho}\,{}^{(2)}t^{\alpha\beta}_{k\bar{k}}(S)$$

$$- \mathscr{S}^{\alpha\beta}(i)\Bigg(\mathscr{S}_{k\bar{k}}(S)\,{}^{(2)}t^{\alpha}_{k}\sum_{S_i=0}^{1}(-1)^{i+S}[i,S_i,S]^{\frac{1}{2}}C(i,S_i,S)\,{}^{(2)}t^{\beta l}_{\varrho\bar{k}}(S_i)$$

$$+ \tfrac{1}{2}[i]^{\frac{1}{2}}\,{}^{(2)}t^{\alpha}_{\varrho}\,{}^{(2)}t^{\beta l}_{\bar{k}k}(S)\Bigg)\Bigg]\delta^{I}_{\sigma} + \mathscr{S}^{\alpha\beta}(i)\Bigg[\mathscr{S}_{\varrho\sigma}(i)\Bigg(\tfrac{1}{2}[i]^{\frac{1}{2}}\,{}^{(1)}t^{\alpha}_{\varrho}\,{}^{(2)}t^{\beta l}_{\bar{k}k}(S)$$

$$+ \mathscr{S}_{k\bar{k}}(S)\delta^{\alpha}_{k}\,{}^{(1)}t^{k'}_{\varrho}\sum_{S_i=0}^{1}(-1)^{i+S}[i,S_i,S]^{\frac{1}{2}}C(i,S_i,S)\,{}^{(2)}t^{\beta l}_{k'\bar{k}}(S_i)\Bigg)\delta^{I}_{\sigma}$$

$$- \delta_{iS}[S]^{-\frac{1}{2}}\,{}^{(1)}t^{\alpha}_{l}\,{}^{(2)}t^{\beta l}_{\bar{k}k}(S)\delta^{l}_{\varrho}\delta^{I}_{\sigma}\Bigg]\Bigg\} - \mathscr{S}_{k\bar{k}}(S)\Bigg\{\mathscr{S}^{\alpha\beta}(i)\Bigg[\delta_{iS}[S]^{-\frac{1}{2}}\,{}^{(2)}t^{\alpha}_{k}\,{}^{(2)}t^{II}_{\varrho\sigma}(S)$$

$$- \mathscr{S}_{\varrho\sigma}(i)\Bigg(\mathscr{S}^{II}(S)\,{}^{(2)}t^{l}_{\varrho}\sum_{S_i=0}^{1}(-1)^{i+S}[i,S_i,S]^{\frac{1}{2}}C(i,S_i,S)\,{}^{(2)}t^{\alpha I}_{\sigma\bar{k}}(S_i)$$

$$+ \tfrac{1}{2}[i]^{\frac{1}{2}}\,{}^{(2)}t^{\alpha}_{\varrho}\,{}^{(2)}t^{\bar{\eta}}_{\sigma k}(S)\Bigg)\Bigg]\delta^{\beta}_{\bar{k}} + \mathscr{S}_{\varrho\sigma}(i)\Bigg[\mathscr{S}^{\alpha\beta}(i)\Bigg(\tfrac{1}{2}[i]^{\frac{1}{2}}\,{}^{(1)}t^{\alpha}_{\varrho}\,{}^{(2)}t^{\bar{\eta}}_{\sigma k}(S)$$

$$+ \mathscr{S}^{II}(S)\delta^{l}_{\varrho}\,{}^{(1)}t^{\alpha}_{l}\sum_{S_i=0}^{1}(-1)^{i+S}[i,S_i,S]^{\frac{1}{2}}C(i,S_i,S)\,{}^{(2)}t^{l'I}_{\sigma k}(S_i)\Bigg)\delta^{\beta}_{\bar{k}}$$

$$- \delta_{iS}[S]^{-\frac{1}{2}}\,{}^{(1)}t^{k'}_{\varrho}\,{}^{(2)}t^{\bar{\eta}}_{\sigma k'}(S)\delta^{\alpha}_{k}\delta^{\beta}_{\bar{k}}\Bigg]\Bigg\}\Bigg). \tag{94}$$

Again, to obtain the final expression for $B^{(1)}_{12}[G^{\alpha\beta}_{\varrho\sigma}(i)]$, we have to set in the above expression $k = \bar{k} = k'$, $l = \bar{l} = l'$ and $S = 0$, and multiply the result by g^{kk}_{II}. This leads to drastic simplification of the terms associated with the diagrams of Fig. 11d and h. Since

$${}^{(2)}t^{\beta l}_{kk}(1) = {}^{(2)}t^{II}_{\sigma k}(1) = 0, \tag{95}$$

the summations over S_i in the expressions corresponding to diagrams $11d_2$ and h_2 reduce to a single term with $S_i = 0$. If we next realize that

$$C(i,0,0) = \tfrac{1}{4}(-1)^{i+1}, \tag{96}$$

$$\mathscr{S}_{\varrho\sigma}(i)\delta^{l}_{\varrho}\delta^{l}_{\sigma} = 2\delta_{i0}\delta^{l}_{\varrho}\delta^{l}_{\sigma}, \tag{97}$$

and

$${}^{(1)}t^{\alpha}_{\varrho}\delta^{l}_{\varrho}\delta^{\alpha}_{k} = {}^{(1)}t^{k}_{l}\delta^{l}_{\varrho}\delta^{\alpha}_{k} = 0, \tag{98}$$

we can rewrite the contribution associated with the three diagrams of Fig. 11d (fourth, fifth and sixth terms in Eq. (94)) as follows:

$$2^{-\frac{3}{2}}[i]^{\frac{1}{2}}N^{\alpha\beta}_{\varrho\sigma}\mathscr{S}^{\alpha\beta}(i)\,{}^{(2)}t^{\beta l}_{kk}(0)\{\mathscr{S}_{\varrho\sigma}(i)({}^{(1)}t^{\alpha}_{\varrho} - {}^{(1)}t^{k}_{\varrho}\delta^{\alpha}_{k})\delta^{l}_{\sigma} - 2\delta_{i0}\,{}^{(1)}t^{\alpha}_{l}\delta^{l}_{\varrho}\delta^{l}_{\sigma}\}$$

$$= 2^{-\frac{3}{2}}[i]^{\frac{1}{2}}N^{\alpha\beta}_{\varrho\sigma}\mathscr{S}^{\alpha\beta}(i)\mathscr{S}_{\varrho\sigma}(i)\,{}^{(1)}t^{\alpha}_{\varrho}\,{}^{(2)}t^{\beta l}_{kk}(0)(1-\delta^{\alpha}_{k}-\delta^{l}_{\varrho})\delta^{l}_{\sigma}$$

$$= 2^{-\frac{3}{2}}[i]^{\frac{1}{2}}N^{\alpha\beta}_{\varrho\sigma}\mathscr{S}^{\alpha\beta}(i)\mathscr{S}_{\varrho\sigma}(i)\,{}^{(1)}t^{\alpha}_{\varrho}\,{}^{(2)}t^{\beta l}_{kk}(0)(1-\delta^{\alpha}_{k})(1-\delta^{l}_{\varrho})\delta^{l}_{\sigma}. \tag{99}$$

Similarly, using Eqs. (96) and (98), and the relation

$$\mathscr{S}^{\alpha\beta}(i)\delta^{\alpha}_{k}\delta^{\beta}_{k} = 2\delta_{i0}\delta^{\alpha}_{k}\delta^{\beta}_{k}, \tag{100}$$

we can replace the contribution corresponding to three diagrams of Fig. 11h (tenth, eleventh and twelfth terms in Eq. (94)) by the expression

$$-2^{-\frac{3}{2}}[i]^{\frac{1}{2}}N^{\alpha\beta}_{\varrho\sigma}\mathscr{S}^{\alpha\beta}(i)\mathscr{S}_{\varrho\sigma}(i)\,{}^{(1)}t^{\alpha}_{\varrho}\,{}^{(2)}t^{ll}_{\sigma k}(0)(1-\delta^{\alpha}_{k})(1-\delta^{l}_{\varrho})\delta^{\beta}_{k}. \tag{101}$$

We thus see that when $k=\bar{k}=k'$, $l=\bar{l}=l'$ and $S=0$, the second and third diagrams in Fig. 11d [11h] eliminate from diagram $11d_1$ [$11h_1$] contributions with $\alpha=k$ and/or $\varrho=l$. This becomes clear when we realize that diagrams $11d_2$, d_3, h_2 and h_3, which are formally connected, can also be interpreted as disconnected terms when k' and l' assume only a single value: Diagram $11d_2$ then cancels the $\alpha=k$ contribution to diagram $11d_1$, while diagram $11d_3$ cancels the contribution with $\varrho=l$. Similar cancellation takes place when we consider diagrams of Fig. 11h. This means that for $k=\bar{k}=k'$, $l=\bar{l}=l'$ and $S=0$, the three diagrams of Fig. 11d and the three diagrams of Fig. 11h may be replaced by single diagrams shown in Figs. 11′d and 11′h, respectively. We thus see that the contribution from the connected diagrams $11d_2$, d_3, h_2 and h_3 can be incorporated into disconnected diagrams $11d_1$ and $11h_1$ by simply adding to the latter ones the numerical factor $(1-\delta^{\alpha}_{k})(1-\delta^{l}_{\varrho})$ (cf. Fig. 11′d,h). This is precisely the factor which appears in expressions (99) and (101).

From Eqs. (94), (99) and (101), and relation (68), it follows that

$$B^{(1)}_{12}[G^{\alpha\beta}_{\varrho\sigma}(i)]=g^{kk}_{ll}\langle\Phi_1|\,{}^{(1)}G^{\alpha\beta}_{\varrho\sigma}(i)T^{(2)}_{2}(T^{(2)}_{1}-T^{(1)}_{1})G^{ll}_{kk}(0)\,|\Phi_1\rangle \tag{102}$$

can be written as

$$\begin{aligned}
B^{(1)}_{12}[G^{\alpha\beta}_{\varrho\sigma}(i)]=2^{-\frac{1}{2}}g^{kk}_{ll}N^{\alpha\beta}_{\varrho\sigma}\Bigg(&\mathscr{S}_{\varrho\sigma}(i)\Bigg\{\delta_{i0}\,{}^{(2)}t^{l}_{\varrho}\,{}^{(2)}t^{\alpha\beta}_{kk}(0)\\
&-\mathscr{S}^{\alpha\beta}(i)\Bigg[{}^{(2)}t^{\alpha}_{k}\sum_{S_i=0}^{1}(-1)^{i}[i,S_i]^{\frac{1}{2}}U(i,S_i)\,{}^{(2)}t^{\beta l}_{\varrho k}(S_i)\\
&+\tfrac{1}{2}[i]^{\frac{1}{2}}({}^{(2)}t^{\alpha}_{\varrho}-{}^{(1)}t^{\alpha}_{\varrho})\,{}^{(2)}t^{\beta l}_{kk}(0)(1-\delta^{\alpha}_{k})(1-\delta^{l}_{\varrho})\Bigg]\Bigg\}\delta^{l}_{\sigma}\\
&-\mathscr{S}^{\alpha\beta}(i)\Bigg\{\delta_{i0}\,{}^{(2)}t^{\alpha}_{k}\,{}^{(2)}t^{ll}_{\varrho\sigma}(0)\\
&-\mathscr{S}_{\varrho\sigma}(i)\Bigg[{}^{(2)}t^{l}_{\varrho}\sum_{S_i=0}^{1}(-1)^{i}[i,S_i]^{\frac{1}{2}}U(i,S_i)\,{}^{(2)}t^{\alpha l}_{\sigma k}(S_i)\\
&+\tfrac{1}{2}[i]^{\frac{1}{2}}({}^{(2)}t^{\alpha}_{\varrho}-{}^{(1)}t^{\alpha}_{\varrho})\,{}^{(2)}t^{ll}_{\sigma k}(0)(1-\delta^{\alpha}_{k})(1-\delta^{l}_{\varrho})\Bigg]\Bigg\}\delta^{\beta}_{k}\Bigg).
\end{aligned} \tag{103}$$

Here, we have also made use of the fact that

$${}^{(2)}t^{\alpha}_{\varrho}={}^{(2)}t^{\alpha}_{\varrho}(1-\delta^{\alpha}_{k})(1-\delta^{l}_{\varrho}). \tag{104}$$

It is clear from Eq. (103) that $B^{(1)}_{12}[G^{\varrho\sigma}_{\alpha\beta}(i)]$ is nonzero only if ${}^{(1)}G^{\varrho\sigma}_{\alpha\beta}(i)$ is equal (up to a permutation of upper or lower indices) to $G^{rl}_{ab}(i)$ or $G^{rs}_{ak}(i)$. In the first case, $B^{(1)}_{12}[G^{\alpha\beta}_{\varrho\sigma}(i)]$ is given by the first four terms in Eq. (103) (the terms appearing between the first pair of curly brackets), while in the second case only the last four terms (appearing between the second pair of curly brackets) give nonvanishing contribution. As explained in [3], disconnected diagrams in Fig. 11a–h and 11′d,h do not generate any disconnected perturbation theory diagrams, since they lead to appearance of the differences ${}^{(2)}t^{a}_{r}-{}^{(1)}t^{a}_{r}$ in the final expression for $B^{(1)}_{12}[G^{\alpha\beta}_{\varrho\sigma}(i)]$. These differences are clearly present in our Eq. (103).

Let us, finally, consider the last of the bilinear coupling terms $\tilde{B}^{(1)}_{12}(G^{\dagger}_{i})$. We can easily verify that no permissible vacuum diagrams can be drawn for the one-body component $\tilde{B}^{(1)}_{12}(G^{\alpha}_{\varrho})$ (the only vacuum diagrams that could be constructed would contain the vertex $T^{(2)}_{2}$ with all lines extending to the right), so that

$$\langle \Phi_1 | {}^{(1)}G^{\alpha}_{\varrho}[T^{(2)}_{2}, T^{(1)}_{1}]\, {}^{(1)}G^{il}_{k\bar{k}}(S) | \Phi_1 \rangle = 0 \tag{105}$$

and

$$\tilde{B}^{(1)}_{12}(G^{\alpha}_{\varrho}) = 0. \tag{106}$$

For the two-body part $\tilde{B}^{(1)}_{12}[G^{\alpha\beta}_{\varrho\sigma}(i)]$, however, we can draw the nonoriented Hugenholtz skeleton shown in Fig. 12. Notice that this is exactly the skeleton (d_2, d_3, h_2, h_3) of Fig. 11. This skeleton is, however, now taken with the plus sign. We can thus expect some cancellations (see the next section for details). Skeleton of Fig. 12 involves a contraction between $T^{(2)}_{2}$ and $T^{(1)}_{1}$. Clearly, such contraction involves only valence orbitals that distinguish references $|\Phi_1\rangle$ and $|\Phi_2\rangle$. In principle, we could also draw skeletons of the type (d_1, h_1) shown in Fig. 11. The corresponding diagrams, however, mutually cancel. The fact that only connected diagrams contribute to $\tilde{B}^{(1)}_{12}[G^{\alpha\beta}_{\varrho\sigma}(i)]$ is associated with the presence of the commutator in Eq. (39).

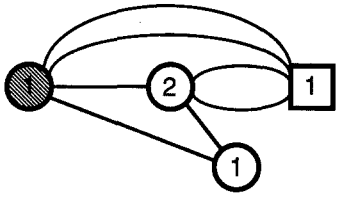

Fig. 12. Nonoriented Hugenholtz skeleton corresponding to $\tilde{B}^{(1)}_{12}[G^{\alpha\beta}_{\varrho\sigma}(i)]$

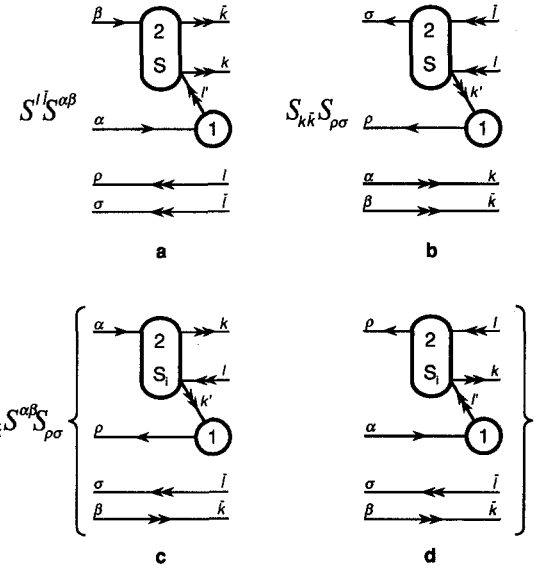

Fig. 12a–d. Brandow diagrams corresponding to $\langle \Phi_1 | {}^{(1)}G^{\alpha\beta}_{\varrho\sigma}(i)[T^{(2)}_{2}, T^{(1)}_{1}]\, {}^{(1)}G^{il}_{k\bar{k}}(S) | \Phi_1 \rangle$. They represent successive terms on the right-hand side of Eq. (107)

Brandow diagrams corresponding to $\tilde{B}^{(1)}_{12}[G^{\alpha\beta}_{\varrho\sigma}(i)]$ or to the matrix element

$$\langle \Phi_1 | {}^{(1)}G^{\alpha\beta}_{\varrho\sigma}(i)[T^{(2)}_2, T^{(1)}_1]\, {}^{(1)}G^{II}_{k\bar{k}}(S) | \Phi_1 \rangle$$

are given in Fig. 12a–d. Clearly, they are identical (except for the minus sign) with the connected diagrams of Fig. 11d and h. The algebraic expression for $\langle \Phi_1 | {}^{(1)}G^{\alpha\beta}_{\varrho\sigma}(i)[T^{(2)}_2, T^{(1)}_1]\, {}^{(1)}G^{II}_{k\bar{k}}(S) | \Phi_1 \rangle$ can be thus written as follows:

$$\begin{aligned}
\langle \Phi_1 | {}^{(1)}G^{\alpha\beta}_{\varrho\sigma}(i)[T^{(2)}_2, T^{(1)}_1]\, {}^{(1)}G^{II}_{k\bar{k}}(S) | \Phi_1 \rangle &= 2^{-\frac{1}{2}} N^{\alpha\beta}_{\varrho\sigma} N^{II}_{k\bar{k}} \\
&\times \Big(\delta_{iS}[S]^{-\frac{1}{2}} \{ \mathscr{S}^{II}(S)[\delta^l_\varrho \delta^I_\sigma] \mathscr{S}^{\alpha\beta}(i)[{}^{(1)}t^{\alpha}_{l'}\, {}^{(2)}t^{\beta l'}_{k\bar{k}}(S)] \\
&- \mathscr{S}_{k\bar{k}}(S)[\delta^\alpha_k \delta^\beta_{\bar{k}}] \mathscr{S}_{\varrho\sigma}(i)[{}^{(1)}t^{k'}_{\varrho}\, {}^{(2)}t^{\bar{I}}_{\sigma k'}(S)] \} \\
&- \sum_{S_i=0}^{1} [i, S_i, S]^{\frac{1}{2}} C(i, S_i, S) \mathscr{S}^{II}(S) \mathscr{S}_{k\bar{k}}(S) \mathscr{S}^{\alpha\beta}(i) \mathscr{S}_{\varrho\sigma}(i) \\
&\times \{ {}^{(1)}t^{k'}_{\varrho}\, {}^{(2)}t^{\alpha l}_{k'k}(S_i) - {}^{(1)}t^{\alpha}_{l'}\, {}^{(2)}t^{l'l}_{\varrho k}(S_i) \} \delta^\beta_{\bar{k}} \delta^I_\sigma \Big).
\end{aligned} \tag{107}$$

This means that the final expression for

$$\tilde{B}^{(1)}_{12}[G^{\alpha\beta}_{\varrho\sigma}(i)] = g^{kk}_{ll} \langle \Phi_1 | {}^{(1)}G^{\alpha\beta}_{\varrho\sigma}(i)[T^{(2)}_2, T^{(1)}_1] G^{ll}_{kk}(0) | \Phi_1 \rangle \tag{108}$$

is

$$\begin{aligned}
\tilde{B}^{(1)}_{12}[G^{\alpha\beta}_{\varrho\sigma}(i)] = 2^{-\frac{1}{2}} g^{kk}_{ll} N^{\alpha\beta}_{\varrho\sigma} \Big(& \delta_{i0} [\delta^l_\varrho \delta^l_\sigma \mathscr{S}^{\alpha\beta}\, {}^{(1)}t^{\alpha}_{l}\, {}^{(2)}t^{\beta l}_{kk}(0) - \delta^\alpha_k \delta^\beta_k \mathscr{S}_{\varrho\sigma}\, {}^{(1)}t^{k}_{\varrho}\, {}^{(2)}t^{ll}_{\sigma k}(0)] \\
& + \tfrac{1}{2}(-1)^i [i]^{\frac{1}{2}} \mathscr{S}^{\alpha\beta}(i) \mathscr{S}_{\varrho\sigma}(i) [{}^{(1)}t^{k}_{\varrho}\, {}^{(2)}t^{\alpha l}_{kk}(0) - {}^{(1)}t^{\alpha}_{l}\, {}^{(2)}t^{ll}_{\varrho k}(0)] \delta^\beta_k \delta^l_\sigma \Big).
\end{aligned} \tag{109}$$

To obtain the above result, we took advantage of the fact that $k' = k$ and $l' = l$ and made use of Eqs. (95) and (96). Clearly, the first term in Eq. (109) contributes only when α, β are core orbitals and $\varrho = \sigma = l$. The second term in Eq. (109) is nonzero only when $\alpha = \beta = k$ and ϱ, σ are virtual orbitals. Finally, the third and fourth terms in Eq. (109) give nonvanishing contributions only when the excitation operator ${}^{(1)}G^{\varrho\sigma}_{\alpha\beta}(i)$ is of the type $G^{rl}_{ak}(i)$.

4. Discussion and comparison with an algebraic approach

Before comparing our results with those obtained using algebraic technique [2, 3], let us discuss the possibility to completely eliminate the connected diagrams of Fig. 12a–d. As mentioned in the previous section, this can be achieved by the mutual cancellation of diagrams $11d_2$ and 12c, $11d_3$ and 12a, $11h_2$ and 12d, and $11h_3$ and 12b. One can easily verify that the remaining diagrams of Fig. 11a–h (i.e. diagrams 11a–c, $11d_1$, 11e–g and $11h_1$), which are collected in Fig. 13a–h, correspond to the matrix element $\langle \Phi_1 | {}^{(1)}G^{\alpha\beta}_{\varrho\sigma}(i)(T^{(2)}_1 - T^{(1)}_1) T^{(2)}_2\, {}^{(1)}G^{II}_{k\bar{k}}(S) | \Phi_1 \rangle$. This is also obvious since

$$T^{(2)}_2 (T^{(2)}_1 - T^{(1)}_1) + [T^{(2)}_2, T^{(1)}_1] = (T^{(2)}_1 - T^{(1)}_1) T^{(2)}_2. \tag{110}$$

Similarly, diagrams 10a and b can be used to represent matrix element

$$\langle \Phi_1 | {}^{(1)}G^{\alpha}_{\varrho}(T^{(2)}_1 - T^{(1)}_1) T^{(2)}_2\, {}^{(1)}G^{II}_{k\bar{k}}(S) | \Phi_1 \rangle,$$

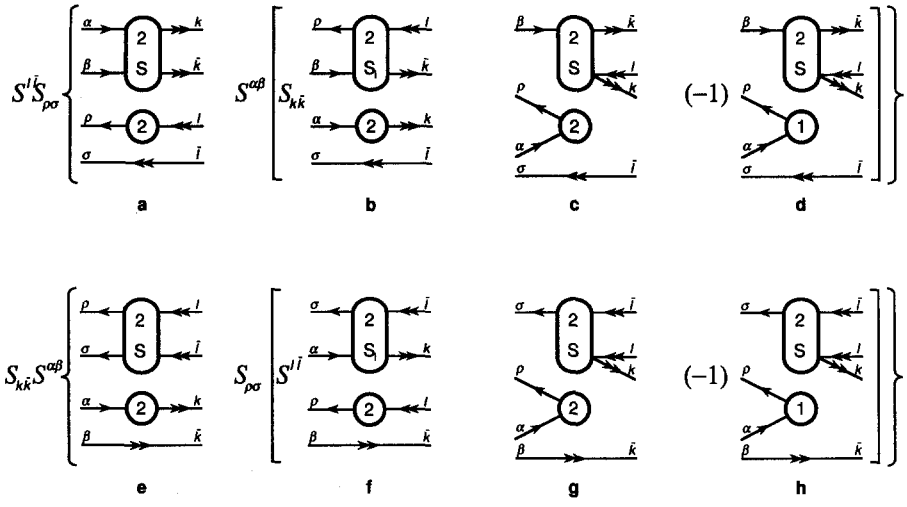

Fig. 13a–h. Brandow diagrams corresponding to $\langle\Phi_1|^{(1)}G^{\alpha\beta}_{\varrho\sigma}(i)(T^{(2)}_1 - T^{(1)}_1)T^{(2)}_2\,{}^{(1)}G^{ll'}_{k\bar{k}}(S)|\Phi_1\rangle$. They are associated with successive terms on the right-hand side of Eq. (113). Minus signs in front of diagrams d and h indicate that the corresponding algebraic expressions have to be subtracted

since [cf. Eq. (91)]

$$\langle\Phi_1|^{(1)}G^{\alpha}_{\varrho}(T^{(2)}_1 - T^{(1)}_1)T^{(2)}_2\,{}^{(1)}G^{ll'}_{k\bar{k}}(S)|\Phi_1\rangle = \langle\Phi_1|^{(1)}G^{\alpha}_{\varrho}T^{(2)}_1T^{(2)}_2\,{}^{(1)}G^{ll'}_{k\bar{k}}(S)|\Phi_1\rangle. \quad (111)$$

We can thus write:

$$\begin{aligned}&\langle\Phi_1|^{(1)}G^{\alpha}_{\varrho}(T^{(2)}_1 - T^{(1)}_1)T^{(2)}_2\,{}^{(1)}G^{ll'}_{k\bar{k}}(S)|\Phi_1\rangle\\ &\quad = -\tfrac{1}{2}N^{ll'}_{k\bar{k}}[\mathscr{S}^{ll'}(S)\,{}^{(2)}t^{l}_{\varrho}\,{}^{(2)}t^{\alpha l'}_{k\bar{k}}(S) + \mathscr{S}_{k\bar{k}}(S)\,{}^{(2)}t^{\alpha}_{k}\,{}^{(2)}t^{ll'}_{\varrho\bar{k}}(S)], \quad (112)\end{aligned}$$

$$\begin{aligned}&\langle\Phi_1|^{(1)}G^{\alpha\beta}_{\varrho\sigma}(i)(T^{(2)}_1 - T^{(1)}_1)T^{(2)}_2\,{}^{(1)}G^{ll'}_{k\bar{k}}(S)|\Phi_1\rangle\\ &= 2^{-\frac{1}{2}}N^{\alpha\beta}_{\varrho\sigma}N^{ll'}_{k\bar{k}}\Bigg(\mathscr{S}^{ll'}(S)\mathscr{S}_{\varrho\sigma}(i)\Bigg\{\delta_{iS}[S]^{-\frac{1}{2}}\,{}^{(2)}t^{l}_{\varrho}\,{}^{(2)}t^{\alpha\beta}_{k\bar{k}}(S)\\ &\quad - \mathscr{S}^{\alpha\beta}(i)\Bigg[\mathscr{S}_{k\bar{k}}(S)\,{}^{(2)}t^{\alpha}_{k}\sum_{S_i=0}^{1}(-1)^{i+S}[i,S_i,S]^{\frac{1}{2}}C(i,S_i,S)\,{}^{(2)}t^{\beta l}_{\varrho\bar{k}}(S_i)\\ &\quad + \tfrac{1}{2}[i]^{\frac{1}{2}}({}^{(2)}t^{\alpha}_{\varrho} - {}^{(1)}t^{\alpha}_{\varrho})\,{}^{(2)}t^{\beta l}_{k\bar{k}}(S)\Bigg]\Bigg\}\delta^{l'}_{\sigma} - \mathscr{S}_{k\bar{k}}(S)\mathscr{S}^{\alpha\beta}(i)\Bigg\{\delta_{iS}[S]^{-\frac{1}{2}}\,{}^{(2)}t^{\alpha}_{k}\,{}^{(2)}t^{ll'}_{\varrho\sigma}(S)\\ &\quad - \mathscr{S}_{\varrho\sigma}(i)\Bigg[\mathscr{S}^{ll'}(S)\,{}^{(2)}t^{l}_{\varrho}\sum_{S_i=0}^{1}(-1)^{i+S}[i,S_i,S]^{\frac{1}{2}}C(i,S_i,S)\,{}^{(2)}t^{\alpha l'}_{\sigma\bar{k}}(S_i)\\ &\quad + \tfrac{1}{2}[i]^{\frac{1}{2}}({}^{(2)}t^{\alpha}_{\varrho} - {}^{(1)}t^{\alpha}_{\varrho})\,{}^{(2)}t^{ll'}_{\sigma\bar{k}}(S)\Bigg]\Bigg\}\delta^{\beta}_{\bar{k}}\Bigg). \quad (113)\end{aligned}$$

It follows from Eqs. (112) and (113) that [cf. Eq. (41)]

$$\begin{aligned}\tilde{\tilde{B}}^{(1)}_{12}(G^{\alpha}_{\varrho}) &= g^{kk}_{ll}\langle\Phi_1|^{(1)}G^{\alpha}_{\varrho}(T^{(2)}_1 - T^{(1)}_1)T^{(2)}_2G^{ll}_{kk}(0)|\Phi_1\rangle\\ &= -\tfrac{1}{2}g^{kk}_{ll}[{}^{(2)}t^{l}_{\varrho}\,{}^{(2)}t^{\alpha l}_{kk}(0) + {}^{(2)}t^{\alpha}_{k}\,{}^{(2)}t^{ll}_{\varrho k}(0)], \quad (114)\end{aligned}$$

and

$$\tilde{\tilde{B}}^{(1)}_{12}[G^{\alpha\beta}_{\varrho\sigma}(i)] = g^{kk}_{ll}\langle\Phi_1|{}^{(1)}G^{\alpha\beta}_{\varrho\sigma}(i)(T^{(2)}_1 - T^{(1)}_1)T^{(2)}_2 G^{ll}_{kk}(0)|\Phi_1\rangle = 2^{-\frac{1}{2}}g^{kk}_{ll}N^{\alpha\beta}_{\varrho\sigma}$$
$$\times\left(\mathscr{S}_{\varrho\sigma}(i)\left\{\delta_{i0}{}^{(2)}t^{l}_{\varrho}{}^{(2)}t^{\alpha\beta}_{kk}(0) - \mathscr{S}^{\alpha\beta}(i)\left[{}^{(2)}t^{\alpha}_{k}\sum_{S_i=0}^{1}(-1)^{i}[i,S_i]^{\frac{1}{2}}U(i,S_i)\,{}^{(2)}t^{\beta l}_{\varrho k}(S_i)\right.\right.\right.$$
$$\left.\left.\left. + \tfrac{1}{2}[i]^{\frac{1}{2}}({}^{(2)}t^{\alpha}_{\varrho} - {}^{(1)}t^{\alpha}_{\varrho})\,{}^{(2)}t^{\beta l}_{kk}(0)\right]\right\}\delta^{l}_{\sigma} - \mathscr{S}^{\alpha\beta}(i)\left\{\delta_{i0}{}^{(2)}t^{\alpha}_{k}{}^{(2)}t^{ll}_{\varrho\sigma}(0)\right.$$
$$- \mathscr{S}_{\varrho\sigma}(i)\left[{}^{(2)}t^{l}_{\varrho}\sum_{S_i=0}^{1}(-1)^{i}[i,S_i]^{\frac{1}{2}}U(i,S_i)\,{}^{(2)}t^{\alpha l}_{\sigma k}(S_i)\right.$$
$$\left.\left.\left. + \tfrac{1}{2}[i]^{\frac{1}{2}}({}^{(2)}t^{\alpha}_{\varrho} - {}^{(1)}t^{\alpha}_{\varrho})\,{}^{(2)}t^{ll}_{\sigma k}(0)\right]\right\}\delta^{\beta}_{k}\right). \tag{115}$$

To obtain Eq. (115), we used the relation (68).

We thus see that from the diagrammatic viewpoint, it is much more convenient to consider the term $\tilde{\tilde{B}}^{(p)}_{12}(G^{\dagger}_i)$, Eqs. (41) and (42), than to examine separately $B^{(p)}_{12}(G^{\dagger}_i)$, Eq. (38), and $\tilde{B}^{(p)}_{12}(G^{\dagger}_i)$, Eq. (39), terms. When $\tilde{\tilde{B}}^{(p)}_{12}(G^{\dagger}_i)$ is used, we do not have to consider the connected diagrams of Fig. 12a–d at all. Consequently, the final expressions for $\tilde{\tilde{B}}^{(p)}_{12}$ are far more compact than the formulas for $B^{(p)}_{12}$ and $\tilde{B}^{(p)}_{12}$. There is, however, some advantage to split $\tilde{\tilde{B}}^{(p)}_{12}$ into $B^{(p)}_{12}$ and $\tilde{B}^{(p)}_{12}$. For example, it is easier to apply the E-operator technique in this case [3]. To some extent, this is due to the fact that the connected terms from $B^{(1)}_{12}[G^{\alpha\beta}_{\varrho\sigma}(i)]$ can be easily incorporated into the terms that are associated with the disconnected diagrams $11d_1$ and h_1 (cf. Fig. 11′d,h). There is also a practical reason for splitting the term $\tilde{\tilde{B}}^{(p)}_{12}$. As mentioned in the preceding section, $B^{(1)}_{12}[G^{\alpha\beta}_{\varrho\sigma}(i)]$ is nonzero when ${}^{(1)}G^{\varrho\sigma}_{\alpha\beta}(i)$ equals $G^{rl}_{ab}(i)$ or $G^{rs}_{ak}(i)$, while $\tilde{\tilde{B}}^{(1)}_{12}[G^{\alpha\beta}_{\varrho\sigma}(i)]$ gives nonvanishing contribution only if ${}^{(1)}G^{\varrho\sigma}_{\alpha\beta}(i)$ is equal to $G^{ll}_{ab}(0)$, $G^{rs}_{kk}(0)$ or $G^{rl}_{ak}(i)$. This means that $B^{(p)}_{12}[G^{\alpha\beta}_{\varrho\sigma}(i)]$ and $\tilde{B}^{(p)}_{12}[G^{\alpha\beta}_{\varrho\sigma}(i)]$ contribute to the coupling term for different types of excitations. It is, therefore, useful from the computational viewpoint to consider $B^{(p)}_{12}(G^{\dagger}_i)$ and $\tilde{B}^{(p)}_{12}(G^{\dagger}_i)$ separately.

Comparing Eq. (114) with Eq. (93) and Eq. (115) with Eq. (103), we see that $\tilde{\tilde{B}}^{(1)}_{12}(G^{\alpha}_{\varrho}) = B^{(1)}_{12}(G^{\alpha}_{\varrho})$, and that there is only a very small difference between the expressions for $\tilde{\tilde{B}}^{(1)}_{12}[G^{\alpha\beta}_{\varrho\sigma}(i)]$ and $B^{(1)}_{12}[G^{\alpha\beta}_{\varrho\sigma}(i)]$, namely, the absence of the factor $(1-\delta^{\alpha}_{k})(1-\delta^{l}_{\varrho})$ in the expression (115) for $\tilde{\tilde{B}}^{(1)}_{12}[G^{\alpha\beta}_{\varrho\sigma}(i)]$. In the preceding section, we have shown that the factor $(1-\delta^{\alpha}_{k})(1-\delta^{l}_{\varrho})$ appears in $B^{(1)}_{12}[G^{\alpha\beta}_{\varrho\sigma}(i)]$ as a result of considering the connected diagrams $11d_2$, d_3, h_2 and h_3. These diagrams are then reintroduced with the opposite sign in the term $\tilde{B}^{(1)}_{12}[G^{\alpha\beta}_{\varrho\sigma}(i)]$, so that the factor $(1-\delta^{\alpha}_{k})(1-\delta^{l}_{\varrho})$ finally disappears and we obtain $\tilde{\tilde{B}}^{(1)}_{12}[G^{\alpha\beta}_{\varrho\sigma}(i)]$. This can also be seen by examining the terms $\mathscr{S}^{\alpha\beta}(i)\mathscr{S}_{\varrho\sigma}(i)({}^{(2)}t^{\alpha}_{\varrho} - {}^{(1)}t^{\alpha}_{\varrho})\,{}^{(2)}t^{\beta l}_{kk}(0)\delta^{l}_{\sigma}$ and $\mathscr{S}^{\alpha\beta}(i)\mathscr{S}_{\varrho\sigma}(i)({}^{(2)}t^{\alpha}_{\varrho} - {}^{(1)}t^{\alpha}_{\varrho})\,{}^{(2)}t^{ll}_{\sigma k}(0)\delta^{\beta}_{k}$, which appear in expression (115). Using the relation [cf. Eqs. (98) and (104)]

$$({}^{(2)}t^{\alpha}_{\varrho} - {}^{(1)}t^{\alpha}_{\varrho})\delta^{\alpha}_{k}\delta^{l}_{\varrho} = 0, \tag{116}$$

we can write

$$\mathscr{S}^{\alpha\beta}(i)\mathscr{S}_{\varrho\sigma}(i)({}^{(2)}t^{\alpha}_{\varrho} - {}^{(1)}t^{\alpha}_{\varrho})\,{}^{(2)}t^{\beta l}_{kk}(0)\delta^{l}_{\sigma} = \mathscr{S}^{\alpha\beta}(i)\mathscr{S}_{\varrho\sigma}(i)({}^{(2)}t^{\alpha}_{\varrho} - {}^{(1)}t^{\alpha}_{\varrho})\,{}^{(2)}t^{\beta l}_{kk}(0)$$
$$\times[(1-\delta^{\alpha}_{k})(1-\delta^{l}_{\varrho}) + \delta^{\alpha}_{k} + \delta^{l}_{\varrho}]\delta^{l}_{\sigma}. \tag{117}$$

Since [cf. Eq. (104)]

$${}^{(2)}t^{k}_{\varrho} = {}^{(2)}t^{\alpha}_{l} = 0, \tag{118}$$

we further obtain

$$\mathcal{S}^{\alpha\beta}(i)\mathcal{S}_{\varrho\sigma}(i)({}^{(2)}t^{\alpha}_{\varrho} - {}^{(1)}t^{\alpha}_{\varrho})\,{}^{(2)}t^{\beta l}_{kk}(0)\delta^{l}_{\sigma}$$
$$= \mathcal{S}^{\alpha\beta}(i)\mathcal{S}_{\varrho\sigma}(i)({}^{(2)}t^{\alpha}_{\varrho} - {}^{(1)}t^{\alpha}_{\varrho})\,{}^{(2)}t^{\beta l}_{kk}(0)(1-\delta^{\alpha}_{k})(1-\delta^{l}_{\varrho})\delta^{l}_{\sigma}$$
$$- \mathcal{S}^{\alpha\beta}(i)\mathcal{S}_{\varrho\sigma}(i)\,{}^{(1)}t^{k}_{\varrho}\,{}^{(2)}t^{\beta l}_{kk}(0)\delta^{\alpha}_{k}\delta^{l}_{\sigma} - \mathcal{S}^{\alpha\beta}(i)\mathcal{S}_{\varrho\sigma}(i)\,{}^{(1)}t^{\alpha}_{l}\,{}^{(2)}t^{\beta l}_{kk}(0)\delta^{l}_{\varrho}\delta^{l}_{\sigma}. \tag{119}$$

Finally, application of Eq. (97) and the obvious property of the (anti)symmetrizers $\mathcal{S}_{\kappa\lambda}(i)$, namely

$$\mathcal{S}_{\kappa\lambda}(i)(\kappa\lambda) = (-1)^{i}\mathcal{S}_{\kappa\lambda}(i), \tag{120}$$

leads to the result

$$\mathcal{S}^{\alpha\beta}(i)\mathcal{S}_{\varrho\sigma}(i)({}^{(2)}t^{\alpha}_{\varrho} - {}^{(1)}t^{\alpha}_{\varrho})\,{}^{(2)}t^{\beta l}_{kk}(0)\delta^{l}_{\sigma}$$
$$= \mathcal{S}^{\alpha\beta}(i)\mathcal{S}_{\varrho\sigma}(i)({}^{(2)}t^{\alpha}_{\varrho} - {}^{(1)}t^{\alpha}_{\varrho})\,{}^{(2)}t^{\beta l}_{kk}(0)(1-\delta^{\alpha}_{k})(1-\delta^{l}_{\varrho})\delta^{l}_{\sigma}$$
$$- (-1)^{i}\mathcal{S}^{\alpha\beta}(i)\mathcal{S}_{\varrho\sigma}(i)\,{}^{(1)}t^{k}_{\varrho}\,{}^{(2)}t^{\alpha l}_{kk}(0)\delta^{\beta}_{k}\delta^{l}_{\sigma} - 2\delta_{i0}\delta^{l}_{\varrho}\delta^{l}_{\sigma}\mathcal{S}^{\alpha\beta}\,{}^{(1)}t^{\alpha}_{l}\,{}^{(2)}t^{\beta l}_{kk}(0). \tag{121}$$

Similarly, we can prove that

$$\mathcal{S}^{\alpha\beta}(i)\mathcal{S}_{\varrho\sigma}(i)({}^{(2)}t^{\alpha}_{\varrho} - {}^{(1)}t^{\alpha}_{\varrho})\,{}^{(2)}t^{ll}_{\sigma k}(0)\delta^{\beta}_{k}$$
$$= \mathcal{S}^{\alpha\beta}(i)\mathcal{S}_{\varrho\sigma}(i)({}^{(2)}t^{\alpha}_{\varrho} - {}^{(1)}t^{\alpha}_{\varrho})\,{}^{(2)}t^{ll}_{\sigma k}(0)(1-\delta^{\alpha}_{k})(1-\delta^{l}_{\varrho})\delta^{\beta}_{k}$$
$$- (-1)^{i}\mathcal{S}^{\alpha\beta}(i)\mathcal{S}_{\varrho\sigma}(i)\,{}^{(1)}t^{\alpha}_{l}\,{}^{(2)}t^{ll}_{\varrho k}(0)\delta^{\beta}_{k}\delta^{l}_{\sigma} - 2\delta_{i0}\delta^{\alpha}_{k}\delta^{\beta}_{k}\mathcal{S}_{\varrho\sigma}\,{}^{(1)}t^{k}_{\varrho}\,{}^{(2)}t^{ll}_{\sigma k}(0). \tag{122}$$

Inserting now Eqs. (121) and (122) into Eq. (115), and using the result of Eq. (103), we obtain

$$\tilde{\tilde{B}}^{(1)}_{12}[G^{\alpha\beta}_{\varrho\sigma}(i)] = B^{(1)}_{12}[G^{\alpha\beta}_{\varrho\sigma}(i)] + 2^{-\frac{1}{2}}g^{kk}_{ll}N^{\alpha\beta}_{\varrho\sigma}$$
$$\times\big(\delta_{i0}\delta^{l}_{\varrho}\delta^{l}_{\sigma}\mathcal{S}^{\alpha\beta}\,{}^{(1)}t^{\alpha}_{l}\,{}^{(2)}t^{\beta l}_{kk}(0) - \delta_{i0}\delta^{\alpha}_{k}\delta^{\beta}_{k}\mathcal{S}_{\varrho\sigma}\,{}^{(1)}t^{k}_{\varrho}\,{}^{(2)}t^{ll}_{\sigma k}(0)$$
$$+\tfrac{1}{2}(-1)^{i}[i]^{\frac{1}{2}}\mathcal{S}^{\alpha\beta}(i)\mathcal{S}_{\varrho\sigma}(i)\,{}^{(1)}t^{k}_{\varrho}\,{}^{(2)}t^{\alpha l}_{kk}(0)\delta^{\beta}_{k}\delta^{l}_{\sigma}$$
$$-\tfrac{1}{2}(-1)^{i}[i]^{\frac{1}{2}}\mathcal{S}^{\alpha\beta}(i)\mathcal{S}_{\varrho\sigma}(i)\,{}^{(1)}t^{\alpha}_{l}\,{}^{(2)}t^{ll}_{\varrho k}(0)\delta^{\beta}_{k}\delta^{l}_{\sigma}\big), \tag{123}$$

so that indeed [see Eq. (109)]

$$\tilde{\tilde{B}}^{(1)}_{12}[G^{\alpha\beta}_{\varrho\sigma}(i)] = B^{(1)}_{12}[G^{\alpha\beta}_{\varrho\sigma}(i)] + \tilde{B}^{(1)}_{12}[G^{\alpha\beta}_{\varrho\sigma}(i)]. \tag{124}$$

Let us now compare the formulas for R, B and $\tilde{B}$ terms derived in Sect. 3 with the expressions obtained in [2, 3]. Let us first examine linear contributions [2].

As implied by the results of Sect. 3, the only linear terms that have to be considered are $R^{(1)}_{1}[G^{ak}_{ll}(0)]$, $R^{(1)}_{1}[G^{kk}_{rl}(0)]$, $R^{(1)}_{2}(G^{a}_{l})$, $R^{(1)}_{2}(G^{k}_{r})$, $R^{(1)}_{2}[G^{ab}_{ll}(0)]$, $R^{(1)}_{2}[G^{kk}_{rs}(0)]$ and $R^{(1)}_{2}[G^{ak}_{rl}(i)]$. The remaining terms $R^{(1)}_{n}(G^{\alpha}_{\varrho})$ and $R^{(1)}_{n}[G^{\alpha\beta}_{\varrho\sigma}(i)]$ $(n=1,2)$ vanish. From Eqs. (62′), (65) and (70) we get:

$$R^{(1)}_{1}[G^{ak}_{ll}(0)] = -g^{kk}_{ll}\,{}^{(2)}t^{a}_{k}, \tag{125}$$

$$R^{(1)}_{1}[G^{kk}_{rl}(0)] = g^{kk}_{ll}\,{}^{(2)}t^{l}_{r}, \tag{126}$$

$$R^{(1)}_{2}(G^{a}_{l}) = -2^{-\frac{1}{2}}g^{kk}_{ll}\,{}^{(2)}t^{al}_{kk}(0), \tag{127}$$

$$R^{(1)}_{2}(G^{k}_{r}) = 2^{-\frac{1}{2}}g^{kk}_{ll}\,{}^{(2)}t^{ll}_{rk}(0), \tag{128}$$

$$R^{(1)}_{2}[G^{ab}_{ll}(0)] = g^{kk}_{ll}N^{ab}_{ll}\,{}^{(2)}t^{ab}_{kk}(0), \tag{129}$$

$$R^{(1)}_{2}[G^{kk}_{rs}(0)] = g^{kk}_{ll}N^{kk}_{rs}\,{}^{(2)}t^{ll}_{rs}(0), \tag{130}$$

$$R^{(1)}_{2}[G^{ak}_{rl}(i)] = g^{kk}_{ll}N^{ak}_{rl}\sum_{S_i=0}^{1}[i,S_i]^{\frac{1}{2}}U(i,S_i)\,{}^{(2)}t^{al}_{rk}(S_i). \tag{131}$$

Thus, employing the relations between the unnormalized and normalized cluster amplitudes [cf. Eqs. (15)–(19)]

$$ {}^{(p)}t_{\varrho}^{\alpha} = \langle \varrho | t_1^{(p)} | \alpha \rangle, \tag{132} $$

$$ {}^{(p)}t_{\varrho\sigma}^{\alpha\beta}(i) = (N_{\varrho\sigma}^{\alpha\beta})^{-1} \langle \varrho\sigma | t_2^{(p)} | \alpha\beta \rangle_i, \tag{133} $$

and the explicit values of the 6-j coefficient $U(X_1, X_2)$ (see Table 1), we obtain:

$$ R_1^{(1)}[G_{ll}^{ak}(0)] = -g_{ll}^{kk} \langle k | t_1^{(2)} | a \rangle, \tag{134} $$

$$ R_1^{(1)}[G_{rl}^{kk}(0)] = g_{ll}^{kk} \langle r | t_1^{(2)} | l \rangle, \tag{135} $$

$$ R_2^{(1)}(G_l^a) = -g_{ll}^{kk} \langle kk | t_2^{(2)} | al \rangle_0, \tag{136} $$

$$ R_2^{(1)}(G_r^k) = g_{ll}^{kk} \langle rk | t_2^{(2)} | ll \rangle_0, \tag{137} $$

$$ R_2^{(1)}[G_{ll}^{ab}(0)] = g_{ll}^{kk} \langle kk | t_2^{(2)} | ab \rangle_0, \tag{138} $$

$$ R_2^{(1)}[G_{rs}^{kk}(0)] = g_{ll}^{kk} \langle rs | t_2^{(2)} | ll \rangle_0, \tag{139} $$

$$ R_2^{(1)}[G_{rl}^{ak}(0)] = -\tfrac{1}{2} g_{ll}^{kk} (\langle rk | t_2^{(2)} | al \rangle_0 - 3^{\frac{1}{2}} \langle rk | t_2^{(2)} | al \rangle_1), \tag{140} $$

$$ R_2^{(1)}[G_{rl}^{ak}(1)] = \tfrac{1}{2} g_{ll}^{kk} (3^{\frac{1}{2}} \langle rk | t_2^{(2)} | al \rangle_0 + \langle rk | t_2^{(2)} | al \rangle_1). \tag{141} $$

Identical expressions are given in Table 3 of [2]. Clearly, the diagrammatic spin-adaptation approach based on graphical methods of angular momentum theory [11, 13b] yields the same results as the E-operator algebraic technique [4]. Our results express, however, the numerical factors entering Eqs. (140) and (141) in terms of the 6-j symbol $U(X_1, X_2)$, Eq. (69).

Let us now turn to bilinear terms. Before comparing our results with those of [3], we point out a different definition of the unnormalized pair-cluster amplitudes and the normalization factors used here (${}^{(p)}t_{\varrho\sigma}^{\alpha\beta}(i)$ and $N_{\alpha\beta}^{\varrho\sigma}$, respectively) and in [3] (${}^{2i+1}t_{\varrho\sigma}^{\alpha\beta}(p)$ and ${}^{2i+1}N_{\alpha\beta}^{\varrho\sigma}$, respectively), namely (see also [16])

$$ {}^{2i+1}N_{\alpha\beta}^{\varrho\sigma} = \tfrac{1}{2}[i]^{-\frac{1}{2}} N_{\alpha\beta}^{\varrho\sigma}, \tag{142} $$

$$ {}^{2i+1}t_{\varrho\sigma}^{\alpha\beta}(p) = [i]^{-\frac{1}{2}} {}^{(p)}t_{\varrho\sigma}^{\alpha\beta}(i). \tag{143} $$

The one-particle cluster amplitudes t_{ϱ}^{α} are the same as in [3].

In [3], the general expression is given only for the component $B_{11}^{(1)}[G_{\varrho\sigma}^{\alpha\beta}(i)]$, while in the remaining cases, only those terms that do not vanish in the special 2-reference case are considered. For example, the connected diagrams corresponding to $B_{12}^{(1)}[G_{\varrho\sigma}^{\alpha\beta}(i)]$ (diagrams $11d_2$, d_3, h_2 and h_3) are not given in [3] and their role in cancelling some disconnected terms (diagrams $11d_1$ and h_1 with $\alpha = k$ or $\varrho = l$) is not commented on, as they do not show up when $G_{\alpha\beta}^{\varrho\sigma}(i)$ equals $G_{ab}^{rl}(i)$ or $G_{ak}^{rs}(i)$ (cf. Sect. 3). For the same reason, the possibility to incorporate the term $\tilde{B}_{12}^{(p)}(G_i^{\dagger})$ in the term $B_{12}^{(p)}(G_i^{\dagger})$ by cancelling the connected diagrams of Fig. 12a–d by the connected diagrams of Fig. 11a–h (the possibility discussed above) is also not considered in [3].

Equivalence of our formula for $B_{11}^{(1)}[G_{\varrho\sigma}^{\alpha\beta}(i)]$, Eq. (75), and of the expression given in [3] is immediately obvious when, in addition to Eq. (142), we apply relations (97), (100), their analogues

$$ \mathscr{S}_{\varrho\sigma}(i)\, {}^{(2)}t_{\varrho}^{l}\, {}^{(2)}t_{\sigma}^{l} = 2\delta_{i0}\, {}^{(2)}t_{\varrho}^{l}\, {}^{(2)}t_{\sigma}^{l}, \tag{144} $$

$$ \mathscr{S}^{\alpha\beta}(i)\, {}^{(2)}t_{k}^{\alpha}\, {}^{(2)}t_{k}^{\beta} = 2\delta_{i0}\, {}^{(2)}t_{k}^{\alpha}\, {}^{(2)}t_{k}^{\beta}, \tag{145} $$

and a simple consequence of the group-theoretical property (120), namely the relation

$$\mathscr{S}^{\alpha\beta}(i)\mathscr{S}_{\varrho\sigma}(i)(\alpha\beta)(\varrho\sigma) = \mathscr{S}^{\alpha\beta}(i)\mathscr{S}_{\varrho\sigma}(i). \tag{146}$$

We use Eqs. (97), (100), (144) and (145) to remove the superfluous symmetrizers $\mathscr{S}^{\alpha\beta}$ and $\mathscr{S}_{\varrho\sigma}$ from the expression given in [3]. This means that our formula for $B_{11}^{(1)}[G_{\varrho\sigma}^{\alpha\beta}(i)]$ is slightly simpler than that given in [3]. This simplification results thanks to the diagrammatic approach, in which the "symmetry forcing" operators $\mathscr{S}^{\alpha\beta}(i)$ and $\mathscr{S}_{\varrho\sigma}(i)$ will appear only when nonequivalent external lines are present in the resulting orbital diagrams [16]. Of course, the resulting formulas for $B_{11}^{(1)}[G_{ll}^{ab}(0)]$, $B_{11}^{(1)}[G_{rs}^{kk}(0)]$ and $B_{11}^{(1)}[G_{rl}^{ak}(i)]$, obtained from the general expression (75), are identical with those given in [3].

According to the results derived in Sect. 3, the remaining types of bilinear terms that have to be considered are $B_{22}^{(1)}[G_{rs}^{ab}(i)]$, $B_{12}^{(1)}(G_r^a)$, $B_{12}^{(1)}[G_{rl}^{ab}(i)]$, $B_{12}^{(1)}[G_{rs}^{ak}(i)]$, $\tilde{B}_{12}^{(1)}[G_{ll}^{ab}(0)]$, $\tilde{B}_{12}^{(1)}[G_{rs}^{kk}(0)]$ and $\tilde{B}_{12}^{(1)}[G_{rl}^{ak}(i)]$. For the components $B_{12}^{(1)}(G_r^a)$, $\tilde{B}_{12}^{(1)}[G_{ll}^{ab}(0)]$, $\tilde{B}_{12}^{(1)}[G_{rs}^{kk}(0)]$ and $\tilde{B}_{12}^{(1)}[G_{rl}^{ak}(i)]$, the equivalence of the results given in [3] and in Sect. 3 is immediately obvious. The only relations that are needed in this case are Eqs. (142) and (143), although in the case of $\tilde{B}_{12}^{(1)}[G_{ll}^{ab}(0)]$ and $\tilde{B}_{12}^{(1)}[G_{rs}^{kk}(0)]$ we must also use Eq. (120), and in the case of $\tilde{B}_{12}^{(1)}[G_{rl}^{ak}(i)]$ we must also realize that for the dichotomic variable X, $X = 0$ or 1, we have

$$2 - [X] = (-1)^X. \tag{147}$$

Only for the components $B_{22}^{(1)}[G_{rs}^{ab}(i)]$, $B_{12}^{(1)}[G_{rl}^{ab}(i)]$ and $B_{12}^{(1)}[G_{rs}^{ak}(i)]$, which are related to the 6-j symbols $U(X_1, X_2)$, Eq. (69), and $V(X_1, X_2, X_3)$, Eq. (88) [see Eqs. (89) and (103)], more complicated relations are needed. This is due to the fact that the 6-j symbols that appear in our expressions arise naturally from the coupling scheme employed, while in the algebraic approach (see Eqs. (29), (33) and (34) of [3]) coupling is implicitly built into the definition of replacement operators and the numerical factors arise through an application of the algebraic version of Wick's theorem. In order to interrelate the resulting factors, we shall rely on the following relations:

$$[X_1] - [X_2] + 1 = 2(-1)^{1+X_1}[X_1]U(X_1, X_2), \tag{148}$$

$$\begin{aligned} &2 - [X_2] - [X_3] + [X_2, X_3] + (2 - [X_1])(2 - [X_2])(2 - [X_3]) \\ &\quad = 4[X_2, X_3]V(X_1, X_2, X_3)^2, \end{aligned} \tag{149}$$

valid for X_i ($i = 1, 2, 3$) that equal 0 or 1. Note that Eq. (148) is a special case of another useful identity [16]:

$$2 - [X_2] - [X_3] + (2 - [X_1])(2 - [X_2])(2 - [X_3]) = -4[X_2, X_3]C(X_1, X_2, X_3). \tag{150}$$

To see this, we set $X_3 = 0$ in Eq. (150), use Eq. (68) and employ the identity

$$1 - [X_1] + (2 - [X_1])(2 - [X_2]) = (-1)^{X_1}(1 + [X_1] - [X_2]), \tag{151}$$

which follows from Eq. (147). Another interesting relation between the 6-j coefficient $V(X_1, X_2, X_3)$, Eq. (88), and the 9-j symbol $C(X_1, X_2, X_3)$, Eq. (67), can be found by comparing Eqs. (149) and (150). In this way we obtain

$$C(X_1, X_2, X_3) + V(X_1, X_2, X_3)^2 = \tfrac{1}{4}. \tag{152}$$

This relation is easy to understand when we realize that the 12-j symbol $R(X_1, X_2, X_3, X_4)$, Eq. (86), satisfies relations [16]

$$\sum_X [X] R(X_1, X_2, X_3, X) = \tfrac{1}{4}, \tag{153}$$

$$\sum_X (-1)^X [X] R(X_1, X_2, X_3, X) = -C(X_1, X_2, X_3), \tag{154}$$

so that [see Eq. (87)]

$$V(X_1, X_2, X_3)^2 = 2R(X_1, X_2, X_3, 0) = \sum_X \{1 + (-1)^X\}[X] R(X_1, X_2, X_3, X)$$
$$= \tfrac{1}{4} - C(X_1, X_2, X_3). \tag{155}$$

In order to see that our expression for $B_{22}^{(1)}[G_{rs}^{ab}(i)]$ [Eq. (89)] is identical with Eq. (29) of [3], we apply Eqs. (142) and (143), and then employ the relation (149). To see that the formulas for $B_{12}^{(1)}[G_{rl}^{ab}(i)]$ and $B_{12}^{(1)}[G_{rs}^{ak}(i)]$, Eqs. (34) and (33) of [3], agree with our general expression for $B_{12}^{(1)}[G_{\varrho\sigma}^{\alpha\beta}(i)]$ [Eq. (103)], we must use Eqs. (142) and (143), identity (148), as well as the relation

$$3 - [X] = 2\delta_{X0}, \tag{156}$$

and equation [16]

$$\mathscr{S}^{\alpha\beta}(i)\, {}^{(2)}t_{\varrho\sigma}^{\alpha\beta}(i) = \mathscr{S}_{\varrho\sigma}(i)\, {}^{(2)}t_{\varrho\sigma}^{\alpha\beta}(i) = 2\, {}^{(2)}t_{\varrho\sigma}^{\alpha\beta}(i), \tag{157}$$

which reflects the symmetry properties of the spin-adapted amplitudes ${}^{(p)}t_{\varrho\sigma}^{\alpha\beta}(i)$ or $\langle \varrho\sigma | t_2^{(p)} | \alpha\beta \rangle_i$ [11], [notice the similarity of Eq. (157) and relations (144) and (145)]. As in the case of $B_{11}^{(1)}[G_{\varrho\sigma}^{\alpha\beta}(i)]$, Eq. (157) enables us to remove the superfluous symmetrizers $\mathscr{S}^{ab}$ and $\mathscr{S}_{rs}$ from the expressions for $B_{12}^{(1)}[G_{rl}^{ab}(i)]$ and $B_{12}^{(1)}[G_{rs}^{ak}(i)]$ given in [3].

We thus see that the diagrammatic spin-adaptation approach based on the graphical methods of angular momentum theory [11, 13b] and the purely algebraic E-operator technique [4] yield equivalent results for both linear, and nonlinear coupling terms appearing in the two-reference coupled cluster theory [2, 3] (there is a misprint in the formula for $B_{12}^{(1)}[G_{rl}^{ab}(i)]$ given in [3]: ${}^1t_{ll}^{ab}(2)$ in the second term of Eq. (34) of [3] should read ${}^1t_{kk}^{ab}(2)$). Although this result was to be expected, direct comparison of the diagrammatic and algebraic methods shows that the formulas obtained with the former technique are slightly simpler. We never have to deal with the superfluous (anti)symmetrizers $\mathscr{S}^{\alpha\beta}(i)$ or $\mathscr{S}_{\varrho\sigma}(i)$, which may result when the algebraic method is used, and we do not have to consider separately the term $\tilde{B}_{12}^{(p)}(G_i^\dagger)$, since it can be easily combined with $B_{12}^{(p)}(G_i^\dagger)$. First of all, however, the algebraic approach does not provide us with the important information about the types of the spin recoupling coefficients, which appear in the spin-adapted expressions, whereas the diagrammatic spin-adaptation approach gives us this information instantaneously. Moreover, the complexity of the calculations does not increase if we apply the diagrammatic technique to higher-order nonlinear terms. Because of the necessity of the evaluation of complicated commutator expressions, calculation of these higher-order terms using the algebraic approach becomes more difficult. Diagrammatic approach should also prove convenient when casting the nonlinear expressions into a recursive form (cf. [18]) that enable an efficient vectorization of the computer code.

Although the diagrammatic method seems to be slightly more convenient than the algebraic technique, it also has some disadvantages, for example, the possibility of overlooking certain diagrams. Moreover, very special care must be exercised to obtain the correct normalization and phase factors. It is, therefore, very important that we can use two entirely different techniques to evaluate the expressions appearing in the orthogonally spin-adapted MR-CC theory. As we have seen in this section, the relationship between the diagrammatic and algebraic spin-adaptation approaches is quite straightforward.

As a final remark, we note that the diagrammatic derivation given in this paper can be easily extended to the case of more than 2-dimensional model spaces, assuming that only closed shell type references are present. In fact, our formulas involve general internal model space excitations ${}^{(1)}G^{\Pi}_{k\bar{k}}(S)$. However, a generalization to an arbitrary model space is far from being straightforward.

Appendix: Spin diagrams and orbital and spin factors associated with coupling terms R, B and $\tilde{B}$

For the sake of completeness and to facilitate an understanding of the results of Sect. 3, we provide in this appendix a complete list of the orbital and spin factors that are associated with Brandow diagrams of Figs. 5a,b, 6a,b, 7a–c, 8a–c, 9a–d, 10a,b, 11a–h and 12a–d and their spin counterparts. The corresponding spin diagrams are presented as well.

One-body components $R^{(1)}_2(G^{\alpha}_{\varrho})$ and $B^{(1)}_{12}(G^{\alpha}_{\varrho})$, that require an evaluation of the matrix elements (63) and (91), are represented by the diagrams of Figs. 6a,b and 10a,b. Algebraic expressions associated with these diagrams take the form:

$$D(G^{\alpha}_{\varrho}; Nx) = N^{\Pi}_{k\bar{k}} \mathscr{S}^{\Pi}(S)^{k^{Nx}_1} \mathscr{S}_{k\bar{k}}(S)^{k^{Nx}_2} \{A(Nx)B(Nx)\}. \tag{A1}$$

Here $D(G^{\alpha}_{\varrho}; Nx)$ is the expression associated with the Brandow diagram of Fig. Nx, $A(Nx)$ designates the pertinent orbital factor (including the orbital sign factor $(-1)^{l+h}$ and the topological weight which always equals 1), and $B(Nx)$ is the spin factor obtained by evaluating the corresponding spin diagram. According to procedure of [16, 17], to evaluate $A(Nx)$ and $B(Nx)$ we use the diagram Nx stripped of the symmetrizers $\mathscr{S}^{\Pi}$ and $\mathscr{S}_{k\bar{k}}$ and only reintroduce the corresponding (anti)symmetrizers $\mathscr{S}^{\Pi}(S)$ and $\mathscr{S}_{k\bar{k}}(S)$ later, i.e. in the final expression. The presence or absence of $\mathscr{S}^{\Pi}(S)$ and $\mathscr{S}_{k\bar{k}}(S)$ in Eq. (A1) is determined by the parameters k^{Nx}_1 and k^{Nx}_2 that are either 0 or 1. Recall that the (anti)symmetrizer $\mathscr{S}^{\Pi}(S)$ [$\mathscr{S}_{k\bar{k}}(S)$] appears only when the external lines l and $\bar{l}$ (k and $\bar{k}$) are nonequivalent, so that two different labelings of external lines l and $\bar{l}$ (k and $\bar{k}$) must be considered.

Orbital and spin factors, $A(Nx)$ and $B(Nx)$, respectively, as well as parameters k^{Nx}_1 and k^{Nx}_2 that determine all one-body contributions $D(G^{\alpha}_{\varrho}; Nx)$, Eq. (A1), are listed in Table 2. As we can see from this table, all spin factors associated with $D(G^{\alpha}_{\varrho}; Nx)$ result from a single spin diagram, which is schematically shown in Fig. 14. Since this diagram separates over the lines S_i and S, it factorizes into a product of two "oyster"-type diagrams (cf., Appendix in [13b]) representing triangular delta functions $\{S_i, \frac{1}{2}, \frac{1}{2}\}$ and $\{S, \frac{1}{2}, \frac{1}{2}\}$ [12]. Consequently, the resulting spin coupling coefficient restricts the summation over the intermediate spin quantum number S_i in every $D(G^{\alpha}_{\varrho}; Nx)$ to only one term $S_i = S$. This summation is already carried out in Brandow diagrams of Figs. 6a,b and 10a,b.

Table 2. Orbital and spin factors, $A(Nx)$ and $B(Nx)$, respectively, spin diagrams and parameters k_i^{Nx}, $i = 1, 2$, determining the one-body contribution $D(G_\varrho^\alpha; Nx)$, Eq. (A1), that is associated with Brandow diagram of Fig. *Nx*

Nx	k_1^{Nx}	k_2^{Nx}	$A(Nx)$	Spin diagram	$B(Nx)$
6a	1	0	$-\delta_\varrho^{I\,(2)}t_{k\bar{k}}^{\alpha I}(S_i)$	14	$2^{-\frac{1}{2}}\delta_{S_iS}$
6b	0	1	$\delta_{\bar{k}}^{\alpha\,(2)}t_{\varrho k}^{\bar{I}I}(S_i)$	14	$2^{-\frac{1}{2}}\delta_{S_iS}$
10a	1	0	$-{}^{(2)}t_{k\bar{k}}^{\alpha I}(S_i)\,{}^{(2)}t_\varrho^I$	14	$\frac{1}{2}\delta_{S_iS}$
10b	0	1	$-{}^{(2)}t_{\varrho\bar{k}}^{\bar{I}I}(S_i)\,{}^{(2)}t_{\bar{k}}^\alpha$	14	$\frac{1}{2}\delta_{S_iS}$

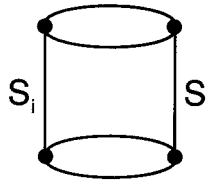

Fig. 14. Spin diagram associated with one-body contributions $D(G_\varrho^\alpha; Nx)$, Eq. (A1). For simplicity, line and vertex orientations are suppressed. The unlabeled lines carry the angular momentum $\frac{1}{2}$

For two-body components we require diagrams in Figs. 5a,b, 7a–c, 8a–c, 9a–d, 11a–h and 12a–d. Algebraic expressions associated with these diagrams have the form:

$$D[G_{\varrho\sigma}^{\alpha\beta}(i); Nx] = N_{\varrho\sigma}^{\alpha\beta}N_{k\bar{k}}^{\bar{I}I}\mathscr{S}^{\bar{I}I}(S)^{k_1^{Nx}}\mathscr{S}_{k\bar{k}}(S)^{k_2^{Nx}}\mathscr{S}^{\alpha\beta}(i)^{k_3^{Nx}}\mathscr{S}_{\varrho\sigma}(i)^{k_4^{Nx}}\{A(Nx)B(Nx)\}, \tag{A2}$$

where Nx, k_i^{Nx}, $A(Nx)$ and $B(Nx)$ have the same meaning as in Eq. (A1) and are listed in Table 3. All nonequivalent spin diagrams that can be associated with Brandow diagrams of Figs. 5a,b, 7a–c, 8a–c, 9a–d, 11a–h and 12a–d are

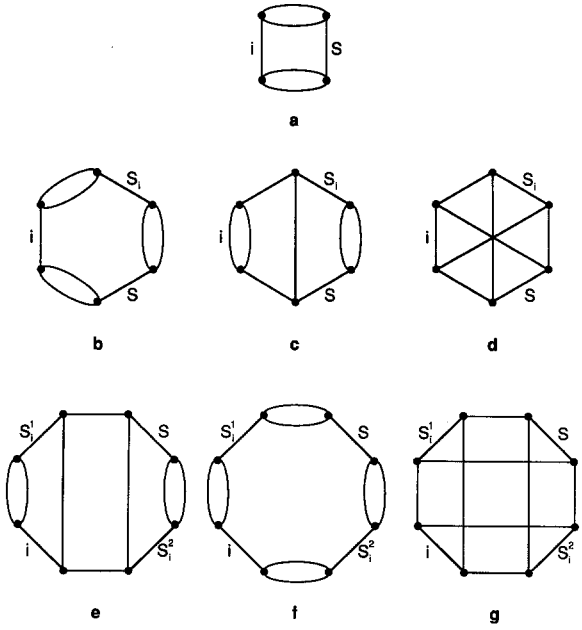

Fig. 15a–g. Spin diagrams associated with two-body contributions $D[G_{\varrho\sigma}^{\alpha\beta}(i); Nx]$, Eq. (A2). As in Fig. 14, line and vertex orientations are suppressed and the unlabeled lines carry the angular momentum $\frac{1}{2}$

Table 3. Orbital and spin factors $A(Nx)$ and $B(Nx)$, respectively, spin diagrams and labels k_i^{Nx}, $i = 1-4$, determining the two-body contribution $D[G_{\varrho\sigma}^{\alpha\beta}(i); Nx]$, Eq. (A2), that is associated with Brandow diagram of Fig. *Nx*

Nx	k_1^{Nx}	k_2^{Nx}	k_3^{Nx}	k_4^{Nx}	$A(Nx)$	Spin diagram	$B(Nx)$
5a	1	1	1	0	$-\delta_\varrho^l \delta_\sigma^\Gamma \delta_k^\beta {}^{(2)}t_k^\alpha$	15a	$2^{-\frac{1}{2}}\delta_{iS}$
5b	1	1	0	1	$\delta_k^\alpha \delta_k^\beta \delta_\sigma^\Gamma {}^{(2)}t_\varrho^l$	15a	$2^{-\frac{1}{2}}\delta_{iS}$
7a	1	0	0	0	$\delta_\varrho^l \delta_\sigma^\Gamma {}^{(2)}t_{kk}^{\alpha\beta}(S_i)$	15b	$\delta_{iS}\delta_{S_iS}[S]^{-\frac{1}{2}}$
7b	0	1	0	0	$\delta_k^\alpha \delta_k^\beta {}^{(2)}t_{\varrho\sigma}^{l\Gamma}(S_i)$	15b	$\delta_{iS}\delta_{S_iS}[S]^{-\frac{1}{2}}$
7c	1	1	1	1	$-\delta_\sigma^\Gamma \delta_k^\beta {}^{(2)}t_{k\varrho}^{\alpha l}(S_i)$	15d	$(-1)^{S_i+1}[i, S_i, S]^{\frac{1}{2}}C(i, S_i, S)$
8a	1	1	0	0	$\delta_\varrho^l \delta_\sigma^\Gamma {}^{(2)}t_k^\alpha {}^{(2)}t_k^\beta$	15a	$\frac{1}{2}\delta_{iS}$
8b	1	1	0	0	$\delta_k^\alpha \delta_k^\beta {}^{(2)}t_\varrho^l {}^{(2)}t_\sigma^\Gamma$	15a	$\frac{1}{2}\delta_{iS}$
8c	1	1	1	1	$-\delta_k^\beta \delta_\sigma^\Gamma {}^{(2)}t_k^\alpha {}^{(2)}t_\varrho^l$	15a	$\frac{1}{2}\delta_{iS}$
9a	1	0	1	0	$-{}^{(2)}t_{\varrho\sigma}^{\alpha l}(S_i^1)\,{}^{(2)}t_{kk}^{\beta\Gamma}(S_i^2)$	15e	$\frac{1}{2}\delta_{iS_i}\delta_{SS_i^2}$
9b	0	1	0	1	$-{}^{(2)}t_{\varrho k}^{\alpha\beta}(S_i^1)\,{}^{(2)}t_{\sigma k}^{l\Gamma}(S_i^2)$	15e	$\frac{1}{2}\delta_{iS_i}\delta_{SS_i^2}$
9c	0	0	0	0	${}^{(2)}t_{kk}^{\alpha\beta}(S_i^1)\,{}^{(2)}t_{\varrho\sigma}^{l\Gamma}(S_i^2)$	15f	$\delta_{iS}\delta_{SS_i^1}\delta_{SS_i^2}[S]^{-1}$
9d	1	1	1	0	${}^{(2)}t_{k\varrho}^{\alpha l}(S_i^1)\,{}^{(2)}t_{k\sigma}^{\beta\Gamma}(S_i^2)$	15g	$(-1)^{S_i^1+S_i^2}[i, S_i^1, S_i^2, S]^{\frac{1}{2}}$ $\times R(i, S_i^1, S_i^2, S)$
11a	1	0	0	1	$\delta_\sigma^\Gamma {}^{(2)}t_\varrho^l {}^{(2)}t_{kk}^{\alpha\beta}(S_i)$	15b	$2^{-\frac{1}{2}}\delta_{iS}\delta_{S_iS}[S]^{-\frac{1}{2}}$
11b	1	1	1	1	$\delta_\sigma^\Gamma {}^{(2)}t_k^\alpha {}^{(2)}t_{k\varrho}^{\beta l}(S_i)$	15d	$2^{-\frac{1}{2}}(-1)^{i+S_i+S+1}$ $\times [i, S_i, S]^{\frac{1}{2}}C(i, S_i, S)$
11c	1	0	1	1	$-\delta_\sigma^\Gamma {}^{(2)}t_\varrho^\alpha {}^{(2)}t_{kk}^{\beta l}(S_i)$	15c	$2^{-\frac{3}{2}}\delta_{S_iS}[i]^{\frac{1}{2}}$
$11d_1$	1	0	1	1	$-\delta_\sigma^\Gamma {}^{(1)}t_\varrho^\alpha {}^{(2)}t_{kk}^{\beta l}(S_i)$	15c	$2^{-\frac{3}{2}}\delta_{S_iS}[i]^{\frac{1}{2}}$
$11d_2$	1	1	1	1	$\delta_k^\alpha \delta_\sigma^\Gamma {}^{(1)}t_\varrho^{k'} {}^{(2)}t_{kk'}^{\beta l}(S_i)$	15d	$2^{-\frac{1}{2}}(-1)^{i+S_i+S+1}$ $\times [i, S_i, S]^{\frac{1}{2}}C(i, S_i, S)$
$11d_3$	1	0	1	0	$\delta_\varrho^l \delta_\sigma^\Gamma {}^{(1)}t_l^\alpha {}^{(2)}t_{kk}^{\beta l}(S_i)$	15b	$2^{-\frac{1}{2}}\delta_{iS}\delta_{S_iS}[S]^{-\frac{1}{2}}$
11e	0	1	1	0	$-\delta_k^\beta {}^{(2)}t_k^\alpha {}^{(2)}t_{\varrho\sigma}^{l\Gamma}(S_i)$	15b	$2^{-\frac{1}{2}}\delta_{iS}\delta_{S_iS}[S]^{-\frac{1}{2}}$
11f	1	1	1	1	$-\delta_k^\beta {}^{(2)}t_\varrho^l {}^{(2)}t_{k\sigma}^{\alpha\Gamma}(S_i)$	15d	$2^{-\frac{1}{2}}(-1)^{i+S_i+S+1}$ $\times [i, S_i, S]^{\frac{1}{2}}C(i, S_i, S)$
11g	0	1	1	1	$\delta_k^\beta {}^{(2)}t_\varrho^\alpha {}^{(2)}t_{\sigma k}^{\Pi}(S_i)$	15c	$2^{-\frac{3}{2}}\delta_{S_iS}[i]^{\frac{1}{2}}$
$11h_1$	0	1	1	1	$\delta_k^\beta {}^{(1)}t_\varrho^\alpha {}^{(2)}t_{\sigma k}^{\Pi}(S_i)$	15c	$2^{-\frac{3}{2}}\delta_{S_iS}[i]^{\frac{1}{2}}$
$11h_2$	1	1	1	1	$-\delta_k^\beta \delta_\varrho^l {}^{(1)}t_l^\alpha {}^{(2)}t_{k\sigma}^{l\Gamma}(S_i)$	15d	$2^{-\frac{1}{2}}(-1)^{i+S_i+S+1}$ $\times [i, S_i, S]^{\frac{1}{2}}C(i, S_i, S)$
$11h_3$	0	1	0	1	$-\delta_k^\alpha \delta_k^\beta {}^{(1)}t_\varrho^{k'} {}^{(2)}t_{\sigma k'}^{\Pi}(S_i)$	15b	$2^{-\frac{1}{2}}\delta_{iS}\delta_{S_iS}[S]^{-\frac{1}{2}}$
12a	1	0	1	0	$\delta_\varrho^l \delta_\sigma^\Gamma {}^{(1)}t_l^\alpha {}^{(2)}t_{kk}^{\beta l}(S_i)$	15b	$2^{-\frac{1}{2}}\delta_{iS}\delta_{S_iS}[S]^{-\frac{1}{2}}$
12b	0	1	0	1	$-\delta_k^\alpha \delta_k^\beta {}^{(1)}t_\varrho^{k'} {}^{(2)}t_{\sigma k'}^{\Pi}(S_i)$	15b	$2^{-\frac{1}{2}}\delta_{iS}\delta_{S_iS}[S]^{-\frac{1}{2}}$
12c	1	1	1	1	$\delta_k^\beta \delta_\sigma^\Gamma {}^{(1)}t_\varrho^{k'} {}^{(2)}t_{kk'}^{\alpha l}(S_i)$	15d	$2^{-\frac{1}{2}}(-1)^{S_i+1}[i, S_i, S]^{\frac{1}{2}}C(i, S_i, S)$
12d	1	1	1	1	$-\delta_k^\beta \delta_\sigma^\Gamma {}^{(1)}t_l^\alpha {}^{(2)}t_{\varrho k}^{l\Gamma}(S_i)$	15d	$2^{-\frac{1}{2}}(-1)^{S_i+1}[i, S_i, S]^{\frac{1}{2}}C(i, S_i, S)$

schematically shown in Fig. 15a–g. The correspondence between the individual orbital diagrams and their spin counterparts can be easily established by comparing the first and the seventh columns of Table 3. Again, to obtain the final expression for a given diagrammatic contribution $D[G_{\varrho\sigma}^{\alpha\beta}(i); Nx]$, we must carry out the summation over the intermediate spin quantum numbers S_i or S_i^1 and S_i^2, which label the orthogonally spin-adapted pair-cluster amplitudes.

As follows from Fig. 15a–g, all spin diagrams corresponding to contributions $D[G^{\alpha\beta}_{\varrho\sigma}(i); Nx]$, except 15d and g, factorize into products of "oyster"-type diagrams. This is true for both the 6-*j* coefficient of Fig. 15a and the 9-*j* coefficients of Figs. 15b and c, as well as for the 12-*j* coefficients of Figs. 15e and f. Thus, in every expression $D[G^{\alpha\beta}_{\varrho\sigma}(i); Nx]$ corresponding to Figs. 15a–c, e and f the summation over the intermediate spin quantum numbers characterizing pair-cluster amplitudes reduces to a single term. Only diagrams 15d and g, which are not separable over $k \leqslant 3$ lines, represent genuine $3n$-*j* coefficients [12]. Diagram 15d represents a 9-*j* symbol $C(i, S_i, S)$, Eq. (67), while the diagram 15e a 12-*j* symbol of the second kind $R(i, S_i^1, S_i^2, S)$, Eq. (86). In expressions $D[G^{\alpha\beta}_{\varrho\sigma}(i); Nx]$, corresponding to these diagrams, the summations over S_i or S_i^1 and S_i^2 remain.

Acknowledgments. Continued research support by NSERC (J.P.) is greatly appreciated. One of us (P.P.) would like to express his sincere gratitude to his co-author, Professor J. Paldus, for his hospitality, thoughtfulness, and numerous helpful discussions during his stay as a Postdoctoral Fellow in the Department of Applied Mathematics of the University of Waterloo.

References

1. Jeziorski B, Monkhorst HJ (1981) Phys Rev A24:1668
2. Jeziorski B, Paldus J (1988) J Chem Phys 88:5673
3. Paldus J, Pylypow L, Jeziorski B (1989) In: Kaldor U (ed) Many-body methods in quantum chemistry. (Lect Notes Chem 52) Springer, Berlin Heidelberg New York, p 151
4. Paldus J, Jeziorski B (1988) Theor Chim Acta 73:81
5. Meissner L (1987) Size extensive methods for the description of electron correlation effects in quasidegenerate states. PhD Thesis, Nicholas Copernicus University, Torun, Poland (in Polish)
6. Meissner L, Jankowski K, Wasilewski J (1988) Int J Quantum Chem 34:535; Meissner L, Jankowski K (1989) ibid 36:705
7. Balková A, Kucharski SA, Meissner L, Bartlett RJ (1991) Theor Chim Acta 80:335
8. Paldus J, Piecuch P, Pylypow L, Jeziorski B, unpublished results
9. Meissner L, Kucharski SA, Bartlett RJ (1989) J Chem Phys 91:6187; Meissner L, Bartlett RJ (1990) J Chem Phys 92:561
10. Paldus J (1983) In: Löwdin PO, Pullman B (eds) New horizons of quantum chemistry. Reidel, Dordrecht, p 31
11. Paldus J (1977) J Chem Phys 67:303; Adams BG, Paldus J (1979) Phys Rev A20:1
12. Jucys AP, Levinson IB, Vanagas VV (1960) Mathematical apparatus of the theory of angular momentum. Institute of Physics and Mathematics of the Academy of Sciences of the Lithuanian S.S.R, Mintis, Vilnius (in Russian); English translations: (1962) Israel Program for Scientific Translations, Jerusalem; (1964) Gordon and Breach, New York; Jucys AP, Bandzaitis AA (1977) The theory of angular momentum in quantum mechanics, 2nd edn. Mokslas, Vilnius (in Russian); Brink DM, Satchler GR (1968) Angular momentum, 2nd edn. Clarendon Press, Oxford; El Baz E, Castel B (1972) Graphical methods of spin algebras in atomic, nuclear and particle physics. Marcel Dekker, New York; for a brief review of these methods, see, e.g., Lindgren I, Morrison J (1982) Atomic many-body theory. Springer, Berlin Heidelberg New York; see also Appendix of Piecuch P (1988) In: Maruani J (ed) Molecules in physics, chemistry and biology, vol 2, Physical aspects of molecular systems. Kluwer, Dordrecht, p 417
13. (a) Čížek J (1966) Theor Chim Acta 6:292; (b) Paldus J, Adams BG, Čížek J (1977) Int J Quantum Chem 11:813
14. Paldus J, Čížek J (1975) Advan Quantum Chem 9:105
15. Harris FE, Jeziorski B, Monkhorst HJ (1981) Phys Rev A23:1632
16. Piecuch P, Paldus J (1989) Int J Quantum Chem 36:429
17. Piecuch P, Paldus J (1990) Theor Chim Acta 78:65
18. Kucharski SA, Bartlett RJ (1991) Theor Chim Acta 80:387